Letters on Materials 16 (1), 2026 pp. 3-22 www.lettersonmaterials.com

Received 12 August 2025; Accepted 7 December 2025
https://doi.org/10.48612/letters/2026-1-3-22 https://elibrary.ru/tqjxlu

Relationship between various enhancement strategies and the quality of joints made by ultrasonic metal welding: A review

Z. Ni†1, J. Ma[1], Z. Yuan[1], A. A. Nazarov[2], J. Yang[3], Y. Wang[4]

†zlni@tju.edu.cn

[1]School of Materials Science and Engineering, North China University of Water Resources and Electric Power, Zhengzhou 450045, China

[2]Institute for Metals Superplasticity Problems, Russian Academy of Sciences, Ufa 450001, Russia

[3]School of Mechatronic Engineering and Automation, Foshan University, Foshan 528225, Guangdong, China

[4]Henan Tianhai Electric Co., Ltd., Hebi 458030, China

Abstract: Ultrasonic metal welding (USMW), a prominent solid-state joining technique, stands out by producing joints with high strength and minimal electrical resistance while consuming far less energy than traditional welding methods. This unique combination makes it particularly well-suited for precision welding of small components and thin metal sheets across various industries. At present, USMW attracts growing attention and adoption within the automotive industry, with a particular surge in applications for new energy vehicles. Its ability to reliably join delicate battery components, conductive materials, and lightweight structures aligns perfectly with the sector's demands for efficiency, durability, and innovation. This paper attempts to summarize the effect of various enhancement strategies employed in UMSW on the mechanical performance of joints, including the process parameter optimization, the weldability between materials and their combinations, the methods of the thermal assistance and implanting interlayer materials between interfaces of the metal sheets. Furthermore, the related application of numerical simulation and online monitoring techniques were introduced, which provided a desirable platform for explaining the joint formation process and improving the welding process robustness. In addition, the mechanism of USMWed interface bonding evolution was discussed in detail. The research results synthesized in this review will provide valuable information for engineers developing USMW systems, researchers exploring related mechanisms, and future studies aiming to advance innovations in the USMW fields.

Keywords: ultrasonic metal welding, enhancement strategies, mechanical performance, joint formation, joint quality

Acknowledgments: *Zenglei Ni was supported by the National Natural Science Foundation of China (No. 52575380, 51905171), Program for Science & Technology Innovation Talents in Universities of Henan Province (No. 24HASTIT045), National Foreign Experts Program (No. S20240015). A.A. Nazarov's work was supported by the State Assignment of the Institute for Metals Superplasticity Problems of the Russian Academy of Sciences (Reg. No. 124022900006-2) financed by the Ministry of Science and Higher Education of the Russian Federation.*

1. Introduction

Ultrasonic metal welding (USMW) is a green and cost-effective technology with great potential for current and future applications. The environmental merits of USMW are significant, as this process does not generate any welding gases or fumes associated with atmospheric warming and environmental pollution. Moreover, USMW technology is very economical and practical due to its advantages of lower energy consumption, high speed, i. e. short welding time, no demands for vacuum, binder as compared to any other welding methods. The origin of USMW can be traced back to the early 1950s, when American researchers conducted experiments on electric resistance spot welding with addition of ultrasonic vibrations. Unexpectedly, they discovered that materials could be joined without the application of welding current and this accidental discovery led to the development of USMW technology [1]. This is a solid-state joining technique which involves frictional motion of the surfaces of sheets under clamping pressure and ultrasonic mechanical vibrations. During this process, surface oxides and contaminants are dispersed under the action of shear and frictional forces to bring the metallic surfaces into contact. As the temperature increases due to frictional heating, the sheet materials experience softening and severe plastic deformation, eventually resulting in the formation of metallurgical bonds [2].

At present, there is still a problem in producing high-quality welds of nonferrous metals via USMW technique due to the lack of high enough tensile properties, hardness and welding stability of the weld joints. In particular, this problem is related to the existence of an upper power limit of the USMW equipment, which directly leads to a low value of the energy transferred to a welding interface making it impossible for the material to undergo enough plastic deformation there [3, 4]. Therefore, to achieve high quality weld joints and improve their mechanical properties, it is essential to induce significant plastic deformation of the materials at a welding interface during USMW. Numerous studies have confirmed that the plastic strain at the welding interface during USMW was mainly affected by welding parameters, such as ultrasonic vibration amplitude, welding power, energy and time, clamping pressure, tool design, etc. [5–10]. Also, the plastic deformation capacity of metals to be welded is determined by microstructural features such as the dislocation structure, precipitated phases, grain size, etc. [11]. Moreover, macroscopic characteristics of the base metals, such as sheet thickness, hardness, surface roughness and oxidation, are also important [12–14]. It is remarkable that a brittle and hard intermetallic layer at interfaces between dissimilar materials is easily formed by USMW despite the low welding temperature, leading to the degradation of mechanical properties [16]. Although this problem cannot be completely avoided, adding an appropriate low melting point material as an interlayer has been shown to effectively enhance the mechanical properties of the joints [15,16]. In fact, the mechanical properties of the welded joints of similar materials can also be enhanced by adding interlayers due to the capacity of promoting material flow, leading to occurrence of larger plastic strain at the weld interface [17,18]. In addition, some prior studies have shown that preheating specimens can significantly improve the joint strength [19], and increasing the welding temperature can enhance the atomic diffusion ability.

To enhance the quality of welds produced during USMW and to better elucidate the bonding mechanisms of welding, several other efforts have been made, including online monitoring, machine learning [20,21], and the dynamic welding process simulation by the finite element modeling. A sound joint can be formed using the methods mentioned above, eliminating the need for direct experimental work.

In view of the above, this article aims to summarize the relationships of welding parameters, interfacial temperature, and deformation behavior with the mechanical properties from the perspective of various kinds of improvement strategies employed during USMW. Moreover, potential future research directions and prospects in this area are identified and discussed at the end of the review.

2. Ultrasonic metal welding system and principles

The key components of a USMW system, as illustrated in Fig. 1 [22], include four main segments: the ultrasonic generator, booster, transducer, and horn. The ultrasonic generator converts the line frequency of 50 Hz or 60 Hz into the operating frequency, which typically ranges from approximately 20 kHz to 120 kHz with high precision [23]. The transducer transforms the high-frequency electrical oscillations into mechanical vibrations of a designed frequency. Mechanical vibrations generated by the transducer are amplified by the booster. Subsequently, the amplified vibrations are transmitted to the horn. Finally, the horn imparts ultrasonic energy to a workpiece clamped between the anvil and horn, thereby completing the welding process [24].

During USMW, energy conversion continuously occurs in the ultrasonic system. That is, electrical energy is transformed to the energy of high-frequency mechanical vibrations. Reciprocal motion of the upper sheet occurs under these vibrations, causing relative friction motions of the surfaces of the two workpieces. Surface oxides and contaminants disperse under the action of shear and frictional forces, leading to the formation of metal-to-metal contacts and joining between the two workpieces [2]. The joint formation process during USMW of two Cu sheets, as shown in Fig. 2.

It is worth mentioning that, although the sonotrode, workpieces, and anvil continuously change their relative positions throughout the different stages of the welding process, a local plastically deformed welding region is ultimately generated between the two workpieces. The specimens, however, remain in a solid state in the entire process, as the material melting point is not reached. Studies show that, for both similar- and dissimilar-metal welding, the process temperatures remain below the melting points of metals. Therefore, compared to traditional fusion welding methods, the formation of intermetallic compounds at the interface is significantly reduced within this temperature range. However, it cannot be completely eliminated, particularly in dissimilar metal welding processes. Consequently, many researchers explore solutions to further reduce the intermetallic compounds and enhance the joint strength, which will be discussed in detail later.

Furthermore, the aforementioned research indicates that the primary issue in the USMW process is the inadequate quality and strength of the joint, primarily resulting from improper welding parameters. Based on a chosen welding configuration, even minor changes can significantly affect the welding process. This will be systematically discussed from two perspectives: machine-dependent and workpiece-dependent factors.

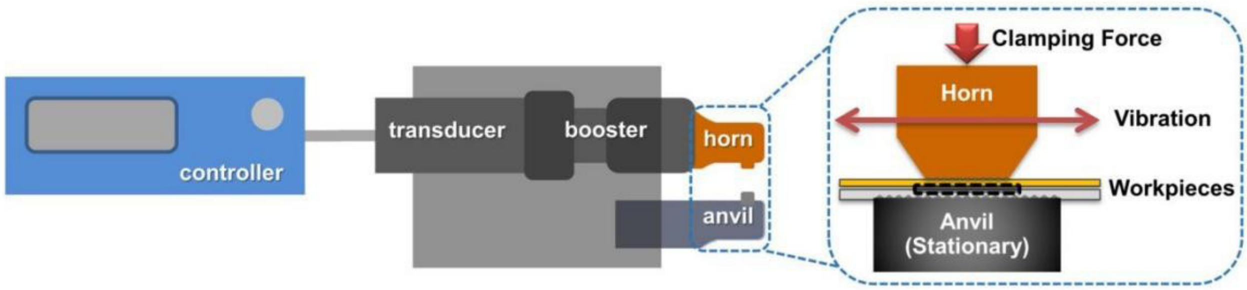

Fig. 1. (Color online) Diagram of an USMW machine [22].

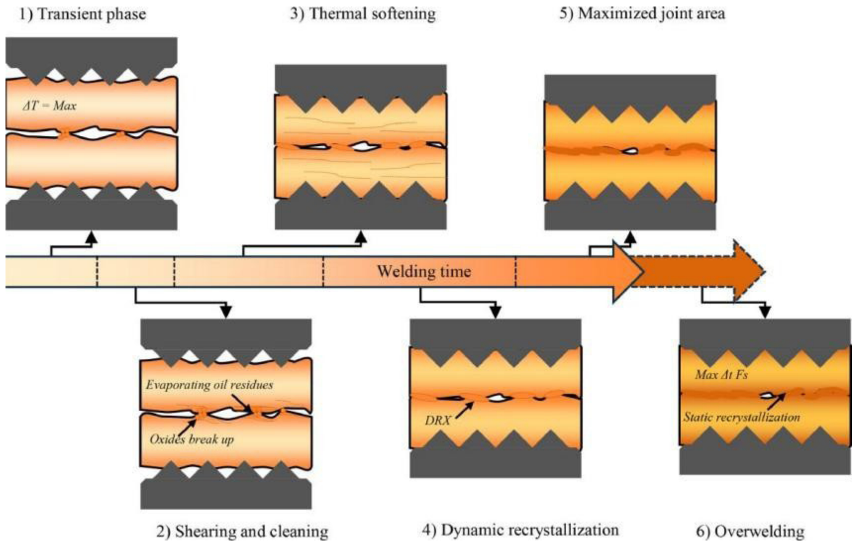

Fig. 2. (Color online) Schematic diagram of joint formation process [23].

3. Equipment parameters optimization approach

The primary process parameters for USMW include ultrasonic frequency, static force, vibration amplitude, welding energy, welding time, peak power, and tooling. Notably, not all of these parameters are independent. For example, USMW machines can be configured to operate in either energy-controlled or time-controlled modes [2]. Consequently, these variables interact with each other during the joint formation process. For instance, altering the welding time effectively adjusts the welding energy input. Specifically, welding energy is the product of power and time. Although most machine-dependent effects remain unchanged without operator intervention, the welding power output typically fluctuates due to the load characteristics. This fluctuation results in a negative correlation between power and welding energy on one hand, and welding time on the other. The relationships among peak power, welding energy, and welding time are illustrated in Fig. 3.

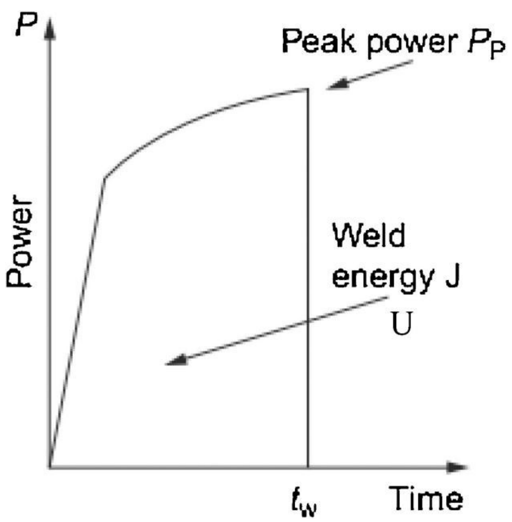

Fig. 3. Relationship among peak power, welding energy and welding time [2].

3.1. Ultrasonic frequency

Ultrasonic vibrations can be generated in two main ways, depending on the power excitation method of an ultrasonic generator. Accordingly, there are two types of ultrasonic generators commonly used: conventional and automatic ones. Conventional ultrasonic generators have gradually become obsolete due to the requirement for manual adjustment of frequency and the difficulty in achieving suitable resonance. In contrast, modern automatic ultrasonic generators feature integrated systems that maintain the transducer at its resonant frequency by regulating the output, which greatly improves welding stability. In other words, the ultrasonic generator must be capable of accurately tracking the changes in the resonant frequency of the ultrasonic transducer in a timely manner. This is one of the important reasons for its growing popularity. As a footnote, note that the ultrasonic frequency refers to the mechanical vibrations generated by the transducer. Typically, depending on the specific ultrasonic systems and application, oscillation frequencies range from 15 to 300 kHz. For instance, welding machines for metallic sheets or wires commonly operate at 20, 30, or 40 kHz, whereas higher frequencies, such as 60 or 150 kHz, are utilized for microjoining applications.

During USMW, the resonant frequency of the vibration system is not constant. Several factors can influence the resonant frequency of the transducer. First of all, machine-related factors such as heating of waveguides during prolonged operation, unstable static pressure, tooling type and wear can affect the resonant frequency. Secondly, the resonant frequency greatly depends on the load changes due to changes of conditions. Heating sample, acoustic softening, sample-to sample changes in the friction conditions at "welding tip-upper sheet", "upper sheet-bottom sheet" and "bottom sheet-anvil" result in the changes of the load from sample to sample and during the welding cycle for a given pair of sheets. Therefore, to compensate these changes and maintain the system at a resonance, the machine generates a range of frequencies and utilizes a feedback control circuit to achieve the frequency modulation, rather than directly generating a fixed frequency. A typical example of the frequency change during welding of copper sheets by welding machine UUSM 6-20 (“Ultra-resonance”, Ekaterinburg, Russia) is presented in Fig. 4.

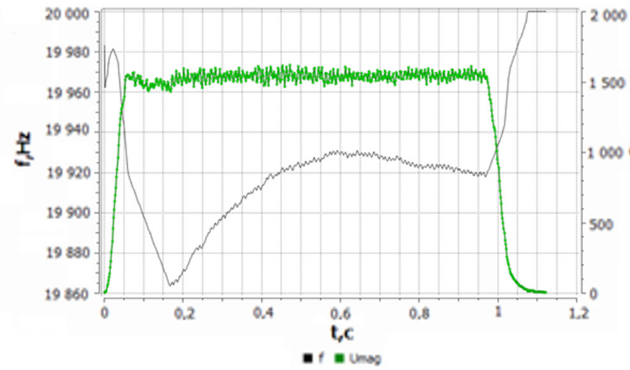

Fig. 4. (Color online) A typical example of welding power (green line) and frequency (black line) changes with time during USMW.

One can see from Fig. 4, despite the changes of welding conditions, the generator supplies fairly constant power, which is due to the very accurate monitoring and appropriate change of the frequency.

Typical USMW machines designed for a nominal working frequency of 20 kHz are equipped with generators capable of producing a range of decided frequencies (say, 19 kHz to 21 kHz) rather than a single frequency (20 kHz). In high-power USMW applications, 20 kHz is a commonly used frequency. At this frequency, high ultrasonic power can generate very high strain rates and strains within less than one second during the shearing of micro asperities at the interface between specimens [24].

3.2. Vibration amplitude

Vibration amplitude is a critical parameter in USMW, as it is directly related to the amount of energy transferred to the welding area. It should be noted that the amplitude of ultrasonic vibration is typically very small. To compare, as the studies have shown, a human hair typically measures between 75 and 100 μm in diameter. So, the vibration amplitudes during UMSW are generally less than the diameter of hairs. As a result, the vibration amplitude is almost imperceptible to the naked eye and can only be accurately measured using highly sensitive instruments, such as displacement sensors [25, 26].

It is important to note that the vibration amplitudes can be measured in two ways, as the peak amplitude (or semi-amplitude) and as the peak-to-peak amplitude. The latter is the difference between the negative and positive peaks of sinusoidal displacement wave. The former is a half of the peak-to-peak amplitude. Peak-to-peak amplitude is the common way of specifying amplitude and commonly the term “amplitude” means it by default.

The vibration amplitude used in welding systems also has two output forms. One form is ultrasonic amplitude as a dependent variable, which varies with the power of the welding system. The other form is ultrasonic amplitude as an independent variable. Due to additional characteristics of a feedback control system, it can be set and controlled at the power supply. The choice depends on the materials and tooling used. The welding amplitude is regulated by the machine’s controller, which sets it as a percentage of the horn’s maximum output [27]. To better illustrate the relationship between these two quantification methods, Shin et al. [25] presented the correlation between the vibration amplitude percentage and the vibration displacement amplitude, as shown in Fig. 5. Similar results were also reported by Feng et al. [26], as exhibited in Fig. 6. In comparison, even if the vibration displacement percentages are at the same levels, the numerical values of the vibration displacements are not the same. This discrepancy is caused by differences in welding equipment and pressure levels.

Note that the variation in ultrasonic amplitude during the welding process serves a dual purpose. Firstly, it can directly affect the joint strength. Secondly, it controls the welding process by influencing other process parameters. Moreover, during USMW, the vibration amplitude of the samples was lower than that of the sonotrode due to an increase in the bonding area. As early as in 2003, Kong et al. [28] reported

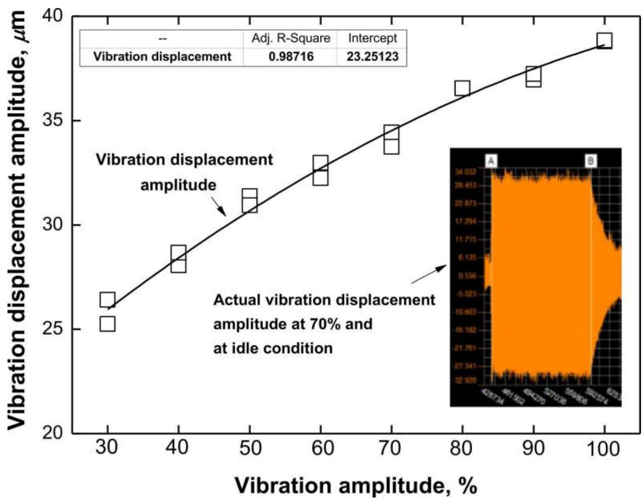

Fig. 5. (Color online) Relationship between the horn vibration displacement amplitude (μm) and the set vibration amplitude (%) [26].

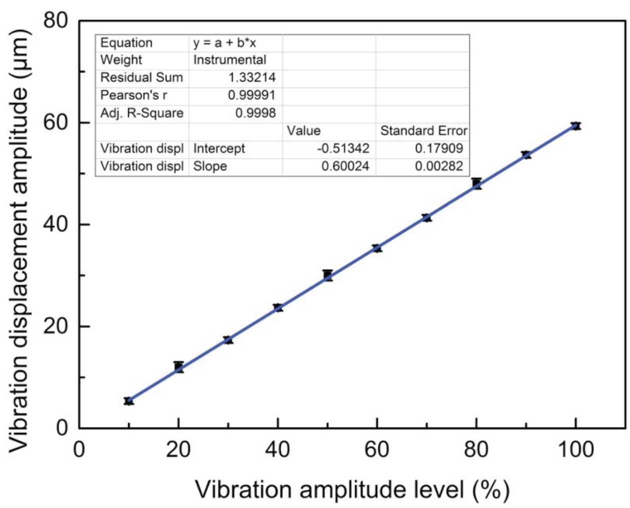

Fig. 6. Relationship between the vibration displacement amplitude and the vibration amplitude level [28].

that the average linear weld density increases approximately linearly as the amplitude rises from 6.8 to 14.3, as shown in Fig. 7. However, the increase in linear weld density has less effect on the improvement of the joints' resistance to peeling.

Park et al. [29] investigated the USMW of copper sheets and evaluated the weldability of the workpiece based on their tensile strength. Samples were produced using amplitude settings in the range of 40% to 80% in 20% increments, welding pressures from 1.5 to 2.5 bar in 0.5 bar increments, and welding times from 0.4 to 0.34 s, recorded every 0.02 s during the welding process. The results indicated that higher numerical percentages of vibration amplitude corresponded to increased tensile strength. Additionally, a threshold point exists at lower levels of vibration amplitude. This indicates that higher vibration amplitudes significantly influence the optimal performance achieved in the USMW of Cu sheets. Kumar et al. [30] employed the combination of experimental and simulation approaches to analyze the effect of ultrasonic amplitude on the joints. The simulation results were consistent with the experimental observations. The analysis indicated that as the ultrasonic amplitude increased, the tensile strength of the joints improved slightly. Therefore, increasing the ultrasonic amplitude can enhance the weldability of the workpieces. Ji et al. [31] investigated the bulk microstructure evolution of USMWed Al foils. Experiments were performed at welding amplitudes of 40%, 60%, and 80% independently, and it was found that the grain size continuously decreased with increasing welding amplitude. The minimum grain size of 25 μm was observed at the highest amplitude of 80%. Elangovan et al. [32] conducted experimental work using conventional USMW equipment (2500 W, 20 kHz) to join Cu sheets with thicknesses of 0.2 mm and 0.3 mm, and also developed mathematical models and performed finite element analysis. The authors employed two welding methods, seam welding and spot welding, for a comparative study of joining Cu sheets. Moreover, prior to the experiments, the specimens were cleaned with acetone to remove impurities. The simulation results agree well with the experimental data, both indicating that the welding interface temperature increases with increasing the amplitude. They explained that the increase of the amplitude facilitated the sliding interactions between the contact areas, leading to significant plastic deformation and increase of the welding interface temperature, as exhibited in Fig. 8. Shin et al. [25] investigated the impact of vibration amplitude on USMW of A5052-H32 alloy sheets. They found that as the vibration amplitude increased, the penetration depth of the horn tip also increased gradually.

Thus, there is a close relationship between the vibration amplitude and bond density. Higher vibration amplitude facilitates effective welding by enabling the workpiece to maintain an optimal interfacial configuration. However, note that only certain ranges of vibration amplitude will yield positive effects. When choosing amplitude, the adhesion between the tooling and the samples should also be considered.

To alleviate the excess tool/part adhesion and the part deformation during USMW, some researchers have used two different amplitude settings during USMW, which was very effective in enhancing the joint strength and appearance quality of the welded material. The transition from the first to the second amplitude setting was controlled by time, energy level, and peak power trigger points, providing an effective method to optimize the initial welding process, known as amplitude stepping. An example of amplitude profiling is shown in Fig. 9 [33].

Baboi et al. [33] compared the mechanical strength with the quality of joints produced using stepped amplitude and constant amplitude modes and found that the amplitude stepping increased the joint strength and reduced the welding time. However, amplitude stepping did not affect the sticking behavior between the tooling and parts, resulting in the absence of any significant improvement in the horn adhesion. This is consistent with the results reported by Al-Sarraf et al. [34].

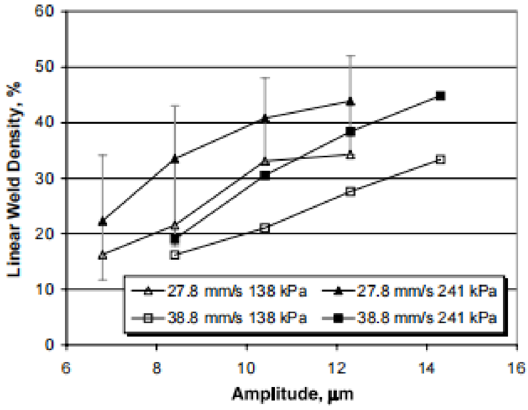

Fig. 7. Effect of welding parameters on linear weld density [28].

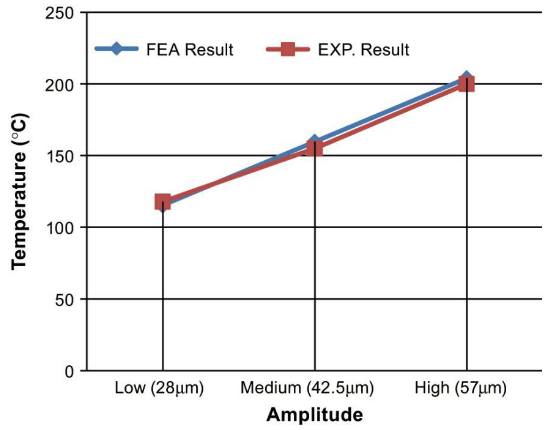

Fig. 8. (Color online) Effect of amplitude on interface temperature during welding of Cu sheets [32].

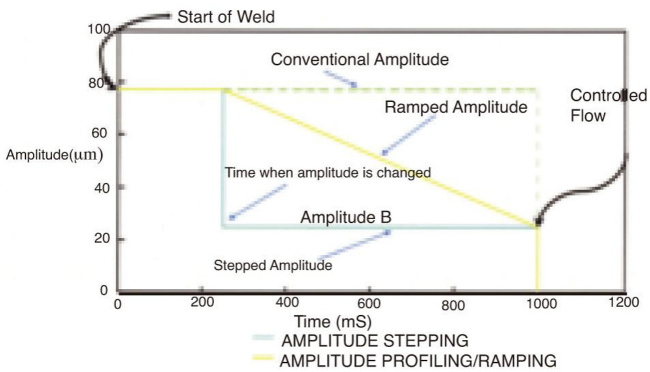

Fig. 9. (Color online) Example of amplitude profiling [33].

3.3. Static force or welding pressure

Static force is a critical parameter in USMW. Its primary function is to press the specimens firmly together, ensuring intimate contact between the components and facilitating the formation of the welded area. This force is applied by the sonotrode tip and anvil, providing the necessary clamping pressure. In USMW, ultrasonic vibration is applied parallel to the workpiece surface, while the static force is always perpendicular to both the vibration direction and the specimen surface. The appropriate value of the static force is selected based on factors, such as material properties, sheet thickness and the welding area. If the clamping pressure is too high, the friction force at the welding interface may exceed the friction between the welding material and the tool, hindering the relative motion of the workpieces and ultimately leading to welding failure. Excessive pressure can also attenuate the vibration amplitude, thereby reducing the strength of the weld joint. Conversely, if the clamping pressure is too low, ultrasonic energy transfer to the specimen is insufficient, resulting in inadequate frictional work. In this case, ultrasonic energy is lost due to surface slippage between the welding tip and the top sheet, causing insufficient deformation at the welding zone and resulting in a weak or even incomplete joint. It was shown that, among various process parameters, welding pressure has the most significant influence on joint properties, followed by welding time and amplitude. Zhu et al. [35] conducted experiments using USMW to join Ti6Al4V and A6061 aluminum alloy sheets, applying welding pressures ranging from 0.3 to 0.5 MPa. The results showed that the optimal welding pressure is 0.4 MPa, at which the effective ultrasonic vibration energy transferred to the specimen via the sonotrode tip is maximized. Shakil et al. [36] employed a 2.4 kW lateral drive USMW system to join 3003 aluminum alloy with 304 stainless steel, investigating the effect of clamping pressure on the mechanical strength of the joints. They observed that, at a welding pressure of 30 psi, increasing the clamping pressure allowed the same level of mechanical strength to be achieved using lower energy input and within a relatively short welding time. Li et al. [37] studied the effect of clamping pressure on the USMW of dissimilar metals joints (Cu/Al sheets) using a combination of experiments and simulations. Their work examined parameters such as vibration amplitude, interface temperature, plastic deformation, intermetallic compound formation, and welding strength. The researchers found that the average vibration amplitude decreases with increasing the welding pressure. Moreover, excessive pressure leads to the extrusion of trace elements from the base material to the interface, which affects interfacial diffusion and promotes the formation of intermetallic compounds, ultimately resulting in poor joint bonding quality. The relationship between the tensile shear strength and clamping force is shown in Fig. 10.

When considering the relationship between pressure and static force, it is important to distinguish between two ways of specifying pressure. In most USMW machines, the static force is supplied by a pneumatic press. The operator can adjust the air pressure within this press, which is often referred to as the “welding pressure”. In contrast, the clamping pressure is the pressure actually exerted on the specimen by the welding tip, which is defined as the clamping force divided by the area of the weld tip.

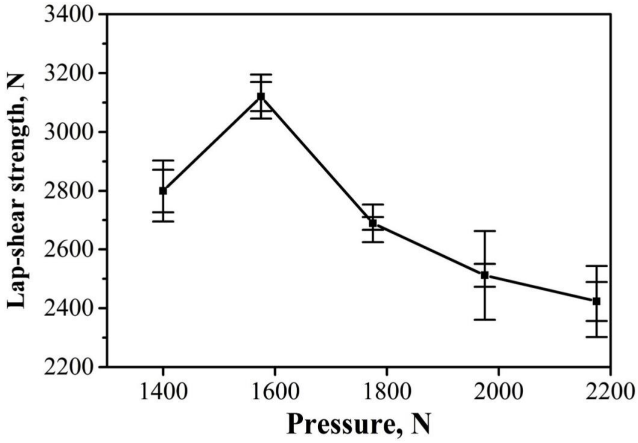

Fig. 10. Lap-shear strength under the various pressure values [37].

3.4. Power, energy and time

The three welding parameters — power, welding time, and energy — are closely interrelated. When the power is constant, the energy input is simply the product of power and welding time. More generally, the energy corresponds to the time-integrated power. Consequently, when evaluating the effects of welding parameters on the mechanical strength of joints produced by USMW, specifying either the welding time or the welding energy may be, to some extent, equivalent. Most of welding machines can operate in any of the two regimes in which either energy or time is set as an independent parameter.

The actual welding power imparted to the welding zone is lower than the one supplied by the ultrasonic generator. The energy losses occur due to the low electromechanical conversion efficiency of the piezoelectric materials, as well as due to the dissipation in the transducer, booster and sonotrode within the ultrasonic system. Accurate measurement of the actual power or energy in the weld zone is very difficult, so their values are estimated by subtracting the consumption during idle vibrations from the total input electrical power. This is also why USMW machines typically offer both energy mode or time mode settings. Increasing the welding time directly increases the total welding energy input, assuming the power remains constant.

The welding energy input directly influences the temperature at the welding interface. The peak temperature is determined by the total welding energy, and the heat is primarily concentrated in the center of the interface rather than on the top surface. As the welding time increases, the extent of material softening also increases, leading to the formation of larger dimples on the joint fracture surface. These larger dimples are indicative of enhanced plasticity. However, excessive welding energy input may cause significant softening, localized melting, or severe stress concentrations due to excessive penetration of the sonotrode tip into the material, which can potentially compromise the integrity of the joint. As early as in 1970, Richter [38] experimentally validated these observations. Macwan et al. [39] investigated

USMW of aluminum to galvanized high-strength low-alloy steel. The tensile lap shear load initially increased with an increase of the welding energy. After reaching its maximum value, the tensile lap shear load decreased with further increasing the welding energy, as illustrated in Fig. 11. This is because, at low welding energy, the plastic deformation of the material is insufficient to achieve full contact at the interaction point, limiting the metal flowability and resulting in the lower joint strength. However, excessive welding energy can damage the base material, significantly reducing the effective thickness of the weld due to the increased material flowability. This reduction of effective thickness decreases the load-carrying capacity, adversely affecting the joint strength. Zhou [6] studied the microstructure and mechanical performance of Al/Ti joints produced by USMW. It was observed that the effective thickness of the joints decreased almost linearly with increasing the welding time, as the sonotrode tip continuously penetrated into the aluminum sheet, thinning the weld zone. Michael et al. [5] investigated the effect of the welding energy input on the mechanical strength of magnesium alloy joints. Results indicate that increasing the welding energy is conductive to the welding interface temperature, promoting the material softening and improving the welding quality. But, excessive welding energy input could result in over-welding and a reduction in the joint quality. Zhao et al. [40] studied the effect of the welding energy on the USMWed Al/Cu joints, and found that the mechanical strength of joints initially increased with increasing the welding energy, peaking at 1000 J before dropping significantly. They observed a swirl-shaped pattern at the welding interface, leading to the mechanical locking between the metals and enhancing the bonding strength. But, cavity defects and intermetallic compounds were more likely to form at the extremely high energy levels. Throughout this process, the failure mode transformed from the interfacial debonding to the nugget pullout and then returned to the cleavage failure.

As study in the field of USMW advances, it has become evident that all possible interactions between process parameters have a significant impact on joint strength. These process parameters are highly interdependent. However, previous studies have primarily focused on their individual effects on joint strength. Consequently, it is crucial to comprehensively consider a range of welding parameters during the actual welding process to optimize the USMW procedure and achieve superior joint quality. USMW is also highly sensitive to variations in surface conditions, such as the presence of contaminants or oxide layers. Importantly, the actual amount of vibration energy delivered during welding can vary from one weld to another, even when all process parameters are held constant. Therefore, energy control is typically employed to minimize inconsistencies in weld quality.

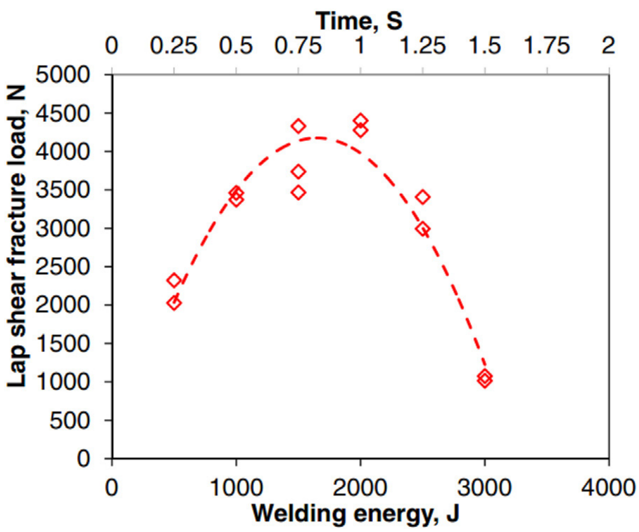

Fig. 11. Effect of the welding energy or welding time on the lap shear load [39].

3.5. Properties of tooling

During USMW, weld formation occurs at the interface between two specimens positioned beneath the sonotrode tip. This process is driven by localized frictional heating generated by the ultrasonic vibration of the sonotrode, which promotes the increased plastic deformation and material flow within the contact region. Therefore, tools should be designed or adjusted to ensure that more energy and vibration can be transferred to the workpiece being welded. Typically, sonotrode tips and anvils with different hardness and roughness values are needed to choose depending on the weld workpieces from various materials for obtaining the optimal USMW performance. These components should be easily replaceable and disassemblable. Tool wear and tear is inevitable in USMW, meaning that there is a maximum number of welds that each tool can fabricate. Once this maximum is reached, it is necessary to replace the sonotrode tip and anvil to prevent a reduction in the effective welding energy delivered to the weld zone. The knurl pattern of the sonotrode tip significantly affects the contact stress and friction coefficient at the interface between the sonotrode tip and the workpieces, thereby playing a crucial role in joint formation. Taking the lap joint as an example, the geometrical design of the knurl pattern on the welding tool surface is primarily determined by the working surfaces, which are subject to wear or adhesion to the metal sheets. Depending on the base material, a protective coating may be required. Material flow occurs more readily beneath the peaks of the sonotrode tip, where higher stress concentration is exerted compared to the valleys. Meanwhile, the purpose of the anvil is to support and secure the workpiece during welding, ensuring efficient transfer of energy and vibration to the material. This enhanced transfer promotes frictional heat generation and facilitates the formation of a strong bond at the weld interface. To facilitate these functions, the interface between the tool and the workpiece is typically machined with knurled patterns consisting of grooves and lands, or other appropriately shaped surface textures. This surface modification increases roughness, thereby improving grip force and reducing relative slippage between the workpiece and the welding tip, which in turn minimizes power losses during welding. Research has shown that the surface patterns of the welding tool play a critical role in influencing both the temperature rise and extent of workpiece adhesion during welding. Shin et al. [25] investigated USMW of A5052-H32 alloy sheets and analyzed three different combinations of horn and anvil patterns, designated as Horns A, B, and C, and Anvils A, B, and C in Fig. 12. Their results indicated that the effect of the horns and anvils on the welding interface temperature and joint mechanical properties were more pronounced than those of the welding parameters, such as amplitude and welding time.

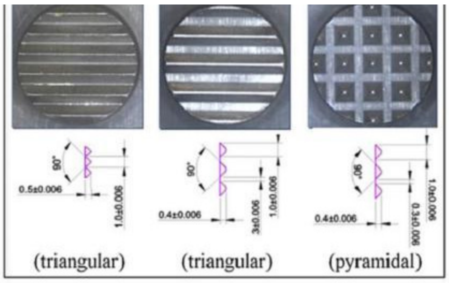

a

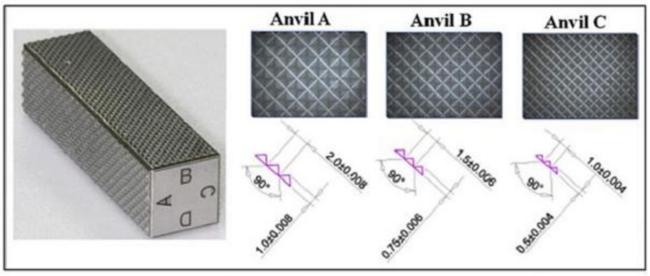

b

Fig. 12. (Color online) Patterns on the surface of the horn (a) and anvil (b) [25].

Nishihara et al. [9] examined the effect of two types of weld tips with different contact face geometries on the mechanical properties of USMWed Al/Fe joints. They found that, under identical welding conditions, joints produced by the cylindrical tip exhibited higher strength than those formed with the flat knurled tip. Feng et al. [26] designed three sonotrode patterns with varying morphologies, including two types of pyramid-shaped teeth with maximum depths of 2.5 mm and 2.0 mm, respectively, as well as quadrangular pyramid-shaped teeth. It was found that the quadrangular pyramid-shaped horn was more conducive to promote the plastic flow between materials, resulting in more effective joining. This finding is consistent with the results of two-dimensional plane model simulation results reported by Lee et al. [10]. To better analyze the tool wear process, Shao et al. [41] summarized the wear variation characteristics of the pyramid-shaped sonotrode tip in both the vibration direction and the perpendicular one. The authors found that, regardless of the direction, the tips of the regular pyramid shape were completely worn down, eventually forming a trapezoidal shape. This finding was consistent with the spatiotemporal modeling of anvil surface evolution reported by Yang et al. [42], as shown in Fig. 13. The complete dataset consists of 19 observations, and the spatiotemporal progression of a part of the anvil surface is illustrated in Fig. 13. However, Jahn et al. [43] reported that USMWed joint of AA6111-T4 aluminum was not significantly influenced by the variations in anvil cap size or knurl patterns.

Nong et al. [12] reported that mechanical properties of joints were significantly improved when a spherical tool was used, as compared to a flat tool, owing to the higher clamping pressures exerted by the spherical tool, which

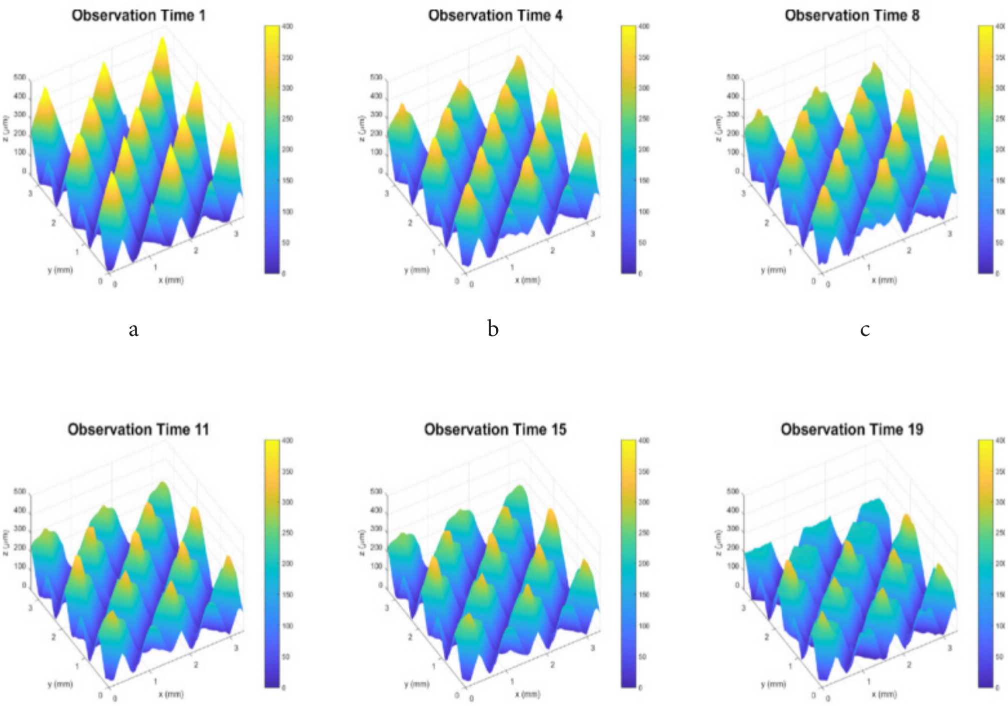

a b c

d e f

Fig. 13. (Color online) Spatiotemporal progression of a part of the anvil surface during USMW: observation time 1 (a), observation time 4 (b), observation time 8 (c), observation time 11 (d), observation time 15 (e) [42].

promoted more severe plastic deformation at the welding interface. Not only are the shapes of the welding tip and anvil knurls important, but their relative positions during welding can also significantly influence the quality of the welds. Murzinova et al. [44] analyzed the relationships between local tensile and compressive strains and the quality of copper joints, and found that compressive strains above 15% are required to achieve high-quality joints. Furthermore, the strain distribution was found to depend on the relative positions of the teeth of the sonotrode tip and the anvil.

With the widespread application of USMW technology, further study is warranted to improve the joint strength by optimizing technological parameters. However, from the overview of the above methods that affect joint quality, it is evident that each parameter affects the weld quality differently. Therefore, it is challenging to establish an optimal set of welding parameters that can be universally applied to all workpiece materials. The best welding parameters for each material can be determined through the minimal testing and optimal experimental design. Improper parameter adjustments can result in under-welding or over-welding. Insufficient pressure can lead to under-welding, which significantly reduces the welding strength. On the other hand, over-welding can cause severe plastic deformation characterized by excessive joint thinning and distortion, leading to cracks propagating along the horn indentation edge.

4. Properties of base metals

The USMW process involves complex material flow and plastic deformation, utilizing mechanical vibration to produce high-quality USMWed joints. With the continuous improvement in the performance requirements of components in the aeronautical and automotive industries, there is an increasing demand for hybrid joints between similar and dissimilar materials. Therefore, the type of materials to be welded must be carefully considered. Key material parameters include elastic modulus, yield strength, hardness, and surface roughness. Softer metals such as Al, Cu, Ni, Mg, Au and Ag, and their alloys are more easily welded ultrasonically, which is attributed to the significant plastic deformation caused by softening during USMW. Studies show that as the material strength and hardness increase, the USMW process becomes more difficult to complete. Additionally, surface roughness can also affect the welding quality.

4.1. Hardness or yield strength

USMW of thin materials, especially those with lower hardness, often results in severe plastic deformation, distortion, and thinning of the samples compared to harder materials, as softer materials are generally more sensitive to ultrasonic vibration energy. However, excessive indentation on the joint surface can negatively affect both the appearance of the parts and their subsequent application. As the yield strength or hardness of the welding material increases, the power required by the USMW equipment increases significantly. This is because the amount of welding energy transmitted to the bonding interface gradually decreases and the degree of material softening is reduced, making it more difficult to ultrasonically weld harder materials. Imai et al. [45] demonstrated that materials with lower hardness facilitate the transmission of vibration energy, thereby making it easier to achieve a high-quality A1050-H24/A1050-O joint by utilizing the softer A1050-O material. On the other hand, the results of USMW for dissimilar materials primarily depend on the hardness differences between the welded specimens. For instance, welding Cu1220 to Al1050 sheets leads to greater plastic deformation in Al than in Cu, regardless of whether the aluminum is on the horn or anvil side, as reported by Shin and De Leon [46]. Similar results were observed by Shin and De Leon [47] in the USMW of Al/Mg joints.

The same material can have different hardness values in different structural states. Of a particular interest is a comparison of the weldability of conventional coarse-grained sheets and the ones with an ultrafine-grained (UFG) structure, i. e. with grain sizes well below 1 μm. UFG materials are much harder than coarse-grained ones at ambient temperatures, but at elevated temperatures they become more ductile. Due to this feature, their weldability can be higher than that of conventional metals. This is confirmed by the recent studies of UMSW of Ni sheets with coarse grained and UFG structures which demonstrated higher lap shear stress of joints of UFG sheets [48]. After UMSW of UFG sheets, gradient microstructure was formed with grain sizes ranging from 3 μm in the bottom sheet to 6 μm in the upper one and 10 μm in the narrow joint zone [49].

Mukhametgalina et al. [50] investigated the microstructure and mechanical properties of the joints of commercially pure Ti. Titanium is much harder than Al and Cu and welding it requires significantly higher energy and temperatures. The authors found that high-quality joints were formed at energy levels that increased the temperature sufficiently to induce α to β phase transformation.

4.2. Thickness

In USMW, the top sheet oscillates along with the sonotrode tip, and heat generation gradually increases due to the interfacial friction between the materials. As the workpiece thickness increases, the loss of acoustic energy transmitted by the welding tip also increases. This reduces the relative motion between the workpieces, resulting in lower interface temperatures and strains. High-quality joints can only be fabricated when the material is sufficiently softened [3]. Therefore, an essential requirement for producing sound joints is that the materials possess an appropriate thickness for welding. Increasing the thickness of the parts, especially those in contact with the sonotrode tip, necessitates a larger sonotrode tip area, higher clamping force, and generally greater welding power. Müller et al. [51] found that reducing the thickness of the top metal sheet typically results in a significantly lower welding energy requirement. At higher energies, excessive welding (over-welding) may occur. Imai et al. [45] reported that the shape of the specimen affects the mechanical strength of the joints, and lower weld strength is observed in specimens with larger sizes or increased thickness.

4.3. Surface roughness

The conditions at the interface between materials are also critical for heat generation during welding. Consequently, even minor variations in surface quality can significantly affect the welding quality. Typically, the decreased surface roughness results in a slower temperature increase at the interface in the later stages of welding, due to the combined action of compression and shear forces. Satpathy and Sahoo [14] investigated the effects of surface roughness and microhardness on bond strength, and concluded that joint strength gradually decreased with increasing surface roughness, as shown in Fig. 14. This phenomenon occurs because excessive surface roughness leads to a progressive reduction in the relative motion between workpieces, weakens the horizontal shear force, and lowers the temperature rise at the interface, ultimately decreasing the degree of plastic deformation. Excessive roughness not only results in unwelded areas, but also impedes plastic deformation, both of which hinder the formation of high-quality joints. However, greater roughness can increase the initial temperature growth rate, as demonstrated by Chen et al. [53].

Mukhametgalina et al. [52] studied the effect of the surface condition of Cu sheets on the quality and strength of joints processed by USMW. Sheets with three different surface states were used: simply washed by alcohol as-received state I with the average roughness $R_a = 0.10$ μm, finely polished state II after grinding with emery paper P1200 ($R_a = 0.10$ μm), and the state III after grinding with coarse paper P240 ($R_a = 0.47$ μm). The peak lap shear load was the highest for the state I and the lowest for state III. Notably, although states I and II exhibited the same surface roughness, the joint strength in state II was lower than in state I, which was attributed to the presence of an oxide film-another critical surface characteristic influencing weld quality.

On the other hand, by establishing a mesoscale model, Huang et al. [54] studied the effects of various surface conditions, such as polishing, filing, and round grinding, on the bonding strength in USMW using multiscale simulations and experimental testing. The results demonstrated that an appropriate increase of roughness could help improve the joint mechanical strength. An appropriate increase in roughness can enhance frictional heat generation during USMW, increase the interface temperature, reduce material flow resistance, and strengthen the "mechanical self-lock" phenomenon of the material at the interface, thereby improving joint strength. Surface treatment of workpieces and appropriate enhancement of material surface roughness are crucial for increasing interface plastic deformation and improving the mechanical bonding strength of joints. Lin et al. [13] investigated the effect of surface roughness on the joining strength of nickel/steel joints. Their results revealed that with mirror-polished surfaces, mechanical strength increased rapidly as welding time increased. However, when the surface roughness of one of the materials was higher, two distinct bonding strength evolution behaviors were observed, and a longer welding time was required to increase the contact fraction and enable the formation of micro-joining areas. The presence of rough surface peaks led to localized clamping stress at limited contact regions, thereby hindering the formation of new contact areas. As a result, the rapid increase in joining strength was delayed until sufficient contact regions were established. Furthermore, improving the roughness on both surfaces further postponed the rapid growth in joining strength, due to the reduced number of effective contact regions formed between the base metals. The influence of surface roughness on the formation of the bonding interface is illustrated in Fig. 15.

5. Thermal preconditioning

To increase the plastic deformation of the weld interface, a convenient method is thermal preconditioning of the material. Preheating can make the temperature distribution at the interface more uniform, enhance welding energy efficiency, and improve the weldability of the material, as reflected in the increased weld area and degree of bonding. Thermal assistance has been proven to be effective in enhancing the quality of various manufacturing processes, primarily through methods such as surface treatment and preheating. This section discusses issues related to material properties and pretreatment methods, as investigated by researchers. Luo et al. [55] investigated the joint formation process under both ambient and preheated conditions. Optical micrographs of joints formed at ambient and preheated states are presented in Fig. 16. The results demonstrated that preheating

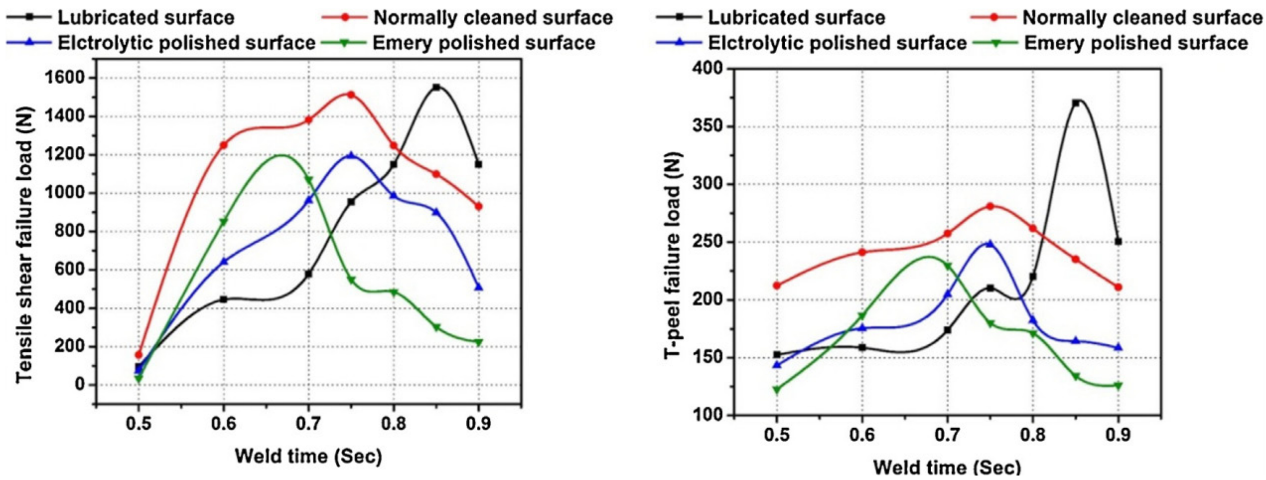

Fig. 14. (Color online) Effects of the surface conditions on the mechanical strength of Al/Cu joints [14].

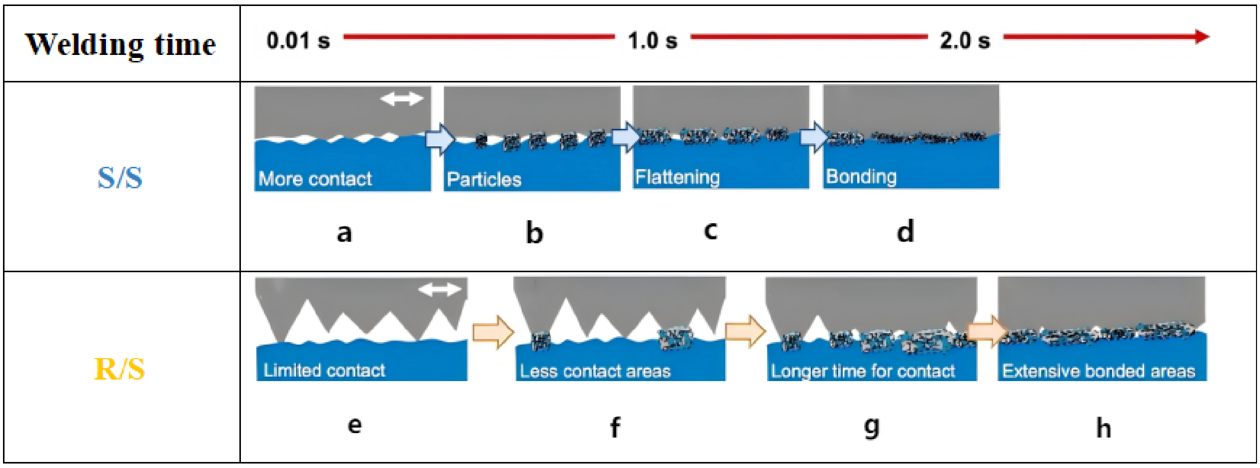

Fig. 15. (Color online) Sketch map of the bonding interface formation process with different surface roughness: smooth/smooth (a – d); rough/smooth (e – g) [13].

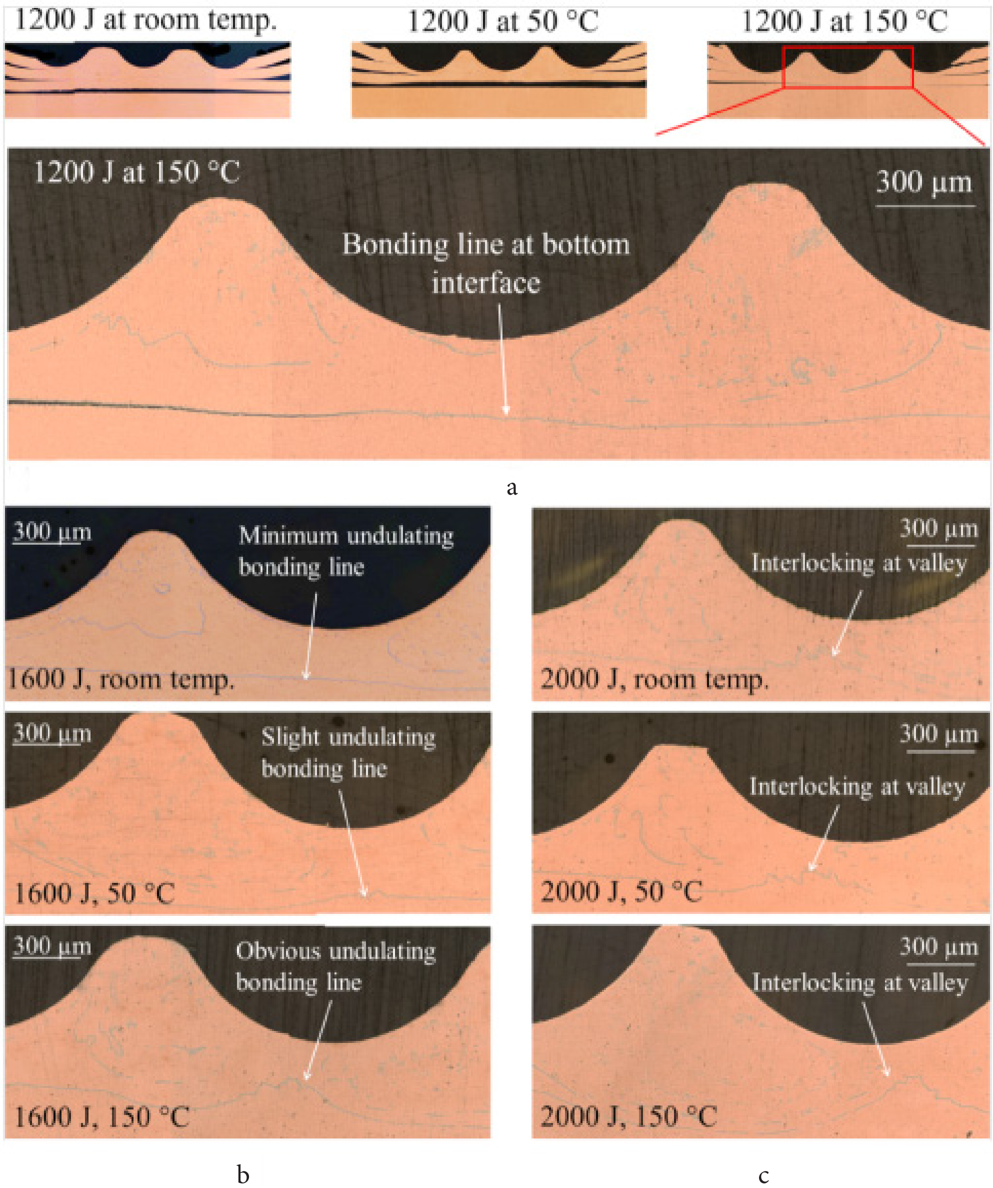

Fig. 16. (Color online) Optical microscopic images of joints under both ambient and preheated conditions with 1200 J (a), 1600 J (b) and 2000 J (c) [55].

significantly enhances joint formation and markedly improves mechanical strength, particularly at the interface closest to the anvil. The beneficial effect of preheating was most pronounced during the initial stage of USMW and gradually decreases as the process continues. Overall, the preheating method can increase the robustness of multilayered joints.

Yang et al. [56] proposed a novel preheating method for workpieces prior to welding. In this technique, a high-intensity direct current (DC) was applied from the sonotrode tip, passed through the faying interface and metal sheets, and conducted into the anvil, generating resistive heat via the Joule effect, as illustrated in Fig. 17. Compared to conventional USMW, DC assistance significantly increased both the peak power and peak temperature, resulting in enhanced material ductility and reduced resistance to plastic deformation. This promoted joint formation during the initial stage of USMW and lead to a substantial improvement in lap shear strength.

Lee et al. [57] conducted thermo-mechanical simulations to investigate vibrations and temperature distributions in USMW Al/Cu multilayered joints. The simulation results indicated that the lowest temperature occurred at the interface between the thicker metal sheet and the anvil. Furthermore, the simulations predicted that preheating could lead to a more uniform temperature distribution across the joint, thereby enhancing weldability at the preheated interfaces.

6. Implanting an interlayer

The mechanical properties of USMWed joints can also be improved by introducing interlayer materials between the joining components. The primary functions of interlayers were to adjust the joint composition, thereby suppressing the growth of interfacial intermetallic compounds and enhancing overall weldability, or to reduce the coefficient of friction at the welding interface, which lowered power consumption. Both effects contributed to an increase in the interface temperature, promoting significant plastic deformation mainly in the vicinity of the joint. Furthermore, interlayers with high plasticity could alleviate local stress concentrations generated during USMW, resulting in joints of superior quality. Interlayer metals were typically classified as either powder or foil types. Therefore, selecting an appropriate interlayer material based on the characteristics of the base metals could effectively enhance joint strength and meet the requirements of engineering applications.

6.1. The type of powder

There are various types of metal powder interlayers, each serving distinct functions. Ni et al. [58] found that increasing the friction coefficient between the two sheets at the welding interface facilitates rapid surface activation. Their experiments showed that employing Al 2219 powder as an interlayer significantly improved the maximum tensile load of Al/Cu joints, achieving a failure load of 73.4 MPa, approximately 2.3 times higher than that of Cu/Al joints without an interlayer (31.8 MPa). Similar findings were reported by Zhang et al. [59]. To better visualize the plastic flow during USMW, Qi et al. [60] introduced interlayers composed of materials different from the base metal, concluding that joints with interlayers exhibited more pronounced plastic flow. Balasundaram et al. [61] investigated USMW of Al/Cu joints using a Zn interlayer, demonstrating that the microhardness of the joint decreased with increasing energy input due to grain growth at elevated temperatures, in line with their earlier findings [62, 63]. Additionally, joints with a Zn interlayer exhibited higher lap shear tensile strength and fracture energy compared to those without the Zn interlayer.

6.2. The type of foils

The foil interlayers at the weld interface can also significantly enhance the mechanical properties of joints. These foils act as buffers, facilitating the atomic diffusion transitions at the interface and minimizing, or even preventing, the formation

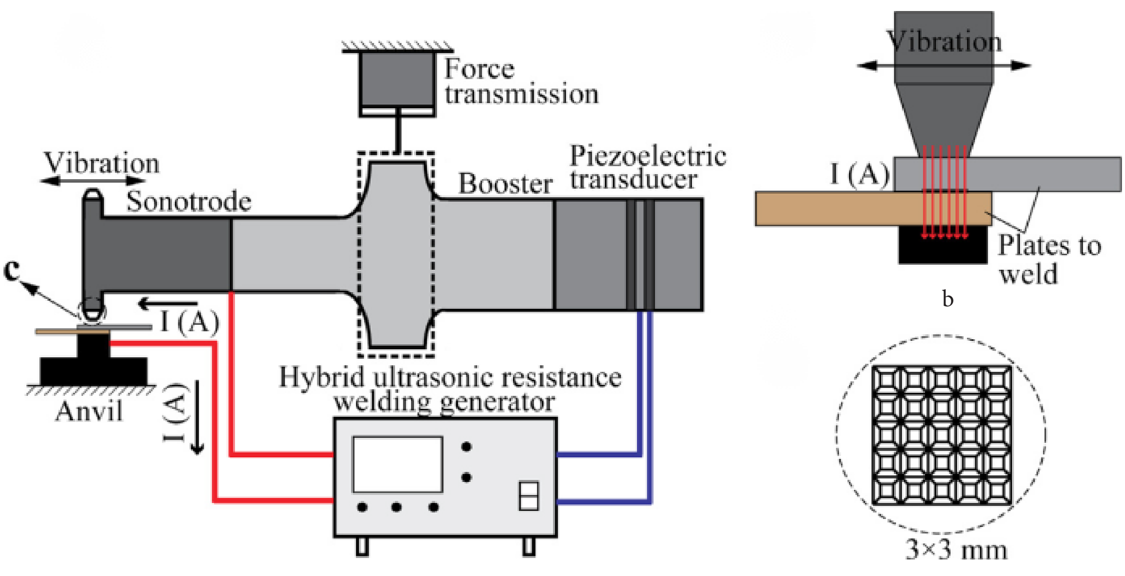

Fig. 17. (Color online) Diagrammatic drawing of the electric Joule effect assisted ultrasonic welding system (a), details of welding location (b) and patterns on the knurled sonotrode tip (c) [56].

of brittle intermetallic compounds, thereby improving the strength of USMWed joints. For example, Ao et al. [64] reported that introducing a 20 μm thick pure Cu foil between a NiTi alloy and stainless steel resulted in a joint strength of 690 N without any detectable intermetallic compounds. Fracture occurred at the NiTi/Cu interface, and the presence of large dimples on the Cu side indicated a ductile fracture mechanism. Peng et al. [65, 66] added Cu and Ag foils, respectively, between Al 6022-T43 and ZEK100-O Mg alloys. Their results showed that the mechanical strength of joints with interlayers increased by at least 31% compared to those without interlayers. The improvement was attributed to the elimination of the undesirable $Mg_{17}Al_{12}$ phase and the formation of an Ag-based solid solution layer, which enhanced the bonding strength. Similarly, Gu et al. [67] introduced a 30 μm thick Zn foil between AZ31B Mg alloy and 6082-T6 Al alloy, boosting joint strength by 90%. This enhancement was ascribed to the formation of beneficial Mg-Zn structures and Zn-Al solid solutions at the interface, instead of the brittle $Al_{12}Mg_{17}$ phase. Further, Lin et al. [68] compared the deformability of Al and Ni interlayers, demonstrating that a highly plastic interlayer promotes material flow at the interface and reduces welding defects. Dash et al. [69] examined the microstructure and mechanical properties of USMWed joints between AA707-clad AA7075-T6 alloy and galvanized high-strength low-alloy (HSLA) steel. The presence of an AA2-clad layer on the Al sheet and a Zn layer on the HSLA sheet suppressed the formation of detrimental intermetallic compounds, resulting in superior shear tensile and fatigue strengths. In addition to metallic foils, coatings can also play a comparable role, similar to the grain deformation effects induced by mechanical grinding, in enhancing the weld interface properties.

6.3. Alcohol and others

Watanabe et al. [70] investigated the effect of adding ethyl alcohol droplets on the tensile load of USMWed A6061-T6/A6061-T6 joints. The ethanol droplets at the weld interface increases the relative movement between the base metal sheets, promotes the generation of higher interface temperatures, and results in a larger welded area. In the absence of ethanol droplets, the number of dimples on the fracture surface decreases, and a new shriveled region becomes evident. The mechanical strength of joints is significantly improved with the addition of ethanol droplets, leading to fracture occurring within the base metal. Similar results were reported by Yang et al. [71]. USMW is a process in which thermal softening effects are observed both at the surface and within the volume of the sheets, facilitating the breakdown of surface oxide layers and other contaminants. However, fractured oxide particles or contaminants may adhere to the welded interface. To achieve optimal weld quality, it is generally effective to remove the oxide film prior to welding, although this is seldom required in USMW due to its tolerance for suboptimal surface conditions. Nevertheless, consistency of surface conditions should be considered. Heymann et al. [72] examined the influence of metal sheet surface condition on USMW process effectiveness, demonstrating that sonotrode adhesion and weld quality are improved when cleaner samples are used. Liu et al. [49] studied the effects of oxides and oils on the mechanical properties of Al/Cu joints fabricated by USMW. The experimental data showed that there was little difference in joint mechanical strength between cleaned and uncleaned interfaces. However, the cleaning procedure increased metallurgical bonding at the welding interface by up to 45%. Since vibration in USMW is only applied to one side of the joint, precise positioning of metal sheets is crucial.

7. Application of information technology

During USMW, the temperature at a welding interface rises rapidly over a short period, resulting in significant plastic deformation of the materials adjacent to the interface. The evolution of the contact interface is highly complex. The small area of the bonding interface makes it challenging to experimentally determine the influence of welding process parameters on the joining mechanism. As a result, finite element modeling (FEM) is commonly employed to simulate the USMW process. Furthermore, real-time in-process monitoring is beneficial for both evaluating weld quality and managing the overall welding system. A well-developed real-time feedback control system can help prevent undesirable variations in weld output and mitigate the risk of system failures. Such systems may incorporate a range of sensors, including pressure and temperature sensors, power and energy input monitors, acoustic sensors, and displacement sensors. By integrating these technologies, weld quality assurance can be enhanced and system reliability maintained.

7.1. Modeling and simulations

This section provides an overview of the development of numerical simulation techniques. Early numerical simulations focused primarily on friction coefficients, rather than considering the combined effects of surface friction and plastic deformation in USMW tools and workpieces. Currently, commercially available FEM software is sufficiently advanced to generate models of stress and strain responses, temperature distribution, and plastic deformation in metal sheets, even at the microstructural level. As a result, these models can provide valuable insights into the joining mechanisms and predict the weld quality. FEM is thus highly effective for estimating the appropriate conditions of joints and provides an efficient means to evaluate whether welding parameters will perform adequately with the chosen materials, without the need for direct experimentation. According to the current study findings, FEM models are commonly developed using an explicit, coupled thermo-mechanical formulation to represent frictional heat generation and temperature distribution at the welding interface. Models with realistic geometric configurations and appropriate computational accuracy are preferred. However, many models restrict their analysis to the sample-tool interface and are limited to short welding times due to model complexity. Additionally, the material parameters are temperature-dependent, and are primarily based on properties such as thermal expansion, thermal conductivity, yield stress, specific heat, plastic strain, and elastic modulus. In contrast, the sonotrode tip and the anvil are typically assumed to be temperature-independent. Therefore, the accuracy of these models is limited by assumptions, such as constant heat input, fixed material thermal properties, a constant friction coefficient, and a single yield strength value. Elangovan et al. [73] developed a model to predict heat generation during the welding of two metal sheets. This model can estimate the elevated temperatures reached in the welding process based on parameters, such as metal sheet thickness, clamping pressure, friction coefficient, and welding time. The authors also explained how material properties, surface conditions, and process variables influence welding behavior. By incorporating the effects of temperature and force during USMW, the model is capable of addressing several challenges that arise during the USMW process.

In contrast, Li et al. [74] developed a three-dimensional (3D) model to investigate the effects of ultrasonic vibrations on the elevated temperature and plastic deformation. Comparisons between simulated and experimental weld cross-sections at various welding times indicated similar trends in thickness changes from the base material as a result of severe plastic deformation. Siddiq and Ghassemi et al. [75] developed a micromechanics-based crystal plasticity model capable of simulating submicron-scale microtexture evolution in materials subjected to ultrasonic vibration. They performed thermo-mechanical analyses to predict frictional heat generation based on a temperature-dependent friction coefficient. The results demonstrated that the friction force at the welding interface was reduced, attributed to both thermal and acoustic softening effects. Shen et al. [76] developed a 3D metallo-thermomechanically coupled FEM model focusing on the microstructure at the welding interface to predict the grain growth and severe plastic deformation under the thermo-mechanical loading conditions. The microstructural evolution during USMW predicted by the model was validated by experimental results with high accuracy. To better understand the fundamental bonding mechanisms, molecular dynamics simulations of USMW were conducted by Yang et al. [77], Shim et al. [78], and Nazarov et al. [79, 80]. These simulations provided a clearer view of the welding process, from atomic diffusion to dislocation formation and temperature variation at the interface, thus revealing the mechanisms underlying joint structure evolution.

7.2. Online monitoring technique and machine learning

The ongoing demand to improve quality and productivity continues to drive advancements during USMW. A critical aspect of this progress is the development of more effective process monitoring and control methods. To ensure that only high-quality battery joints proceed to subsequent production stages, achieving near-zero misdetection rates in monitoring the welding process is essential. Current research efforts focus on measuring and visualizing the effects of process parameters and individual disturbances during USMW. Statistical investigations employing machine learning have also been successfully conducted to analyze the influence of welding parameters on joint mechanical strength. However, identifying suitable monitoring tools and establishing reliable correlations between their outputs and USMW outcomes or corresponding models remains a persistent challenge. While ultrasonic welding machines are commonly equipped with built-in system monitoring capabilities, users can typically collect data on power consumption and sonotrode displacement. Nevertheless, linking these measurements directly to joint quality remains complex. However, these metrics can be utilized to detect missing wires or sheets in a stack-up, as variations in displacement values may indicate such defects. Excessive power consumption may signal a material or mechanical issue that leads to poor joint quality, but pinpointing the exact cause remains challenging [67]. As previously discussed and further demonstrated by Zhao et al. [25], thermal monitoring has remained a primary inspection method due to the wide range of available sensors. Mongan et al. [21] confirmed the effectiveness of machine learning in predicting the mechanical strength of joints between steel and aluminum specimens. Meng et al. [81] demonstrated that machine learning-based response surface methods can simultaneously optimize welding parameters under multiple load cases, such as shear and T-peel strength. Mantra [82] and Zhao et al. [20, 83] utilized artificial neural networks to develop analytical models based on process parameters. Welding variables, including clamping pressure, time and amplitude, were used as inputs to the artificial neural network to create a training model capable of predicting joint mechanical strength under various welding conditions. However, this approach typically requires a large number of experiments to obtain the prior data necessary for training an accurate prediction model. To address this issue, Yang et al. [84] proposed a novel response surface modeling method based on hybrid multi-task learning, which enhances the predictive performance of response surface models without increasing experimental costs.

8. Mechanical properties

It is essential to evaluate USMWed joints under conditions that closely resemble real-life applications. Weld strength, which reflects the mechanical performance of the joint, is a key indicator of overall weld quality. Consequently, ensuring safety is a fundamental requirement for products that utilize USMW.

8.1. Evaluation of weld strength and failure mode

The strength of a joint is characterized by its maximum load-carrying capacity before failure occurs. Testing is typically conducted under quasi-static loading conditions. The U-tensile test is used to assess the joint's normal strength, the lap-shear test evaluates shear strength, and the T-peel test measures a combination of both normal and shear strength. Both U-tensile and T-peel testing will damage the joint, highlighting the importance of finding a new method to evaluate USMWed joints using nondestructive testing. The resulting failure modes, which are commonly associated with the weld strength, can be commonly utilized to identify the weld strength. The typical failure modes include complete pull-out failure, interfacial failure, and mixed failure. Complete pull-out failure is generally categorized as an over weld due to the excessive thinning and distortion of the joints, resulting in the cracks propagating along the horn indentation. Interfacial failure is considered as a form of underwelding, as debonding initiates and propagates along the weld interface, which is typically associated with low mechanical strength. Mixed failure is a combination of the aforementioned modes, where fracture often originates at the weld interface and extends through the thickness of the base metal. This failure mode generally results in relatively high weld strength, and such joints are commonly regarded as having sound quality. In general, two critical conditions should be considered when analyzing these three failure modes. First, material waviness or elemental diffusion should be present at the weld interface. Second, the differences in material properties between the metal sheets should be minimal. Typical tensile shear load (N)-displacement (mm) curves as a function of welding energy are shown in Fig. 18.

8.2. Hardness distribution

To provide a better illustration of the hardness distribution at the welding interface, many researchers segment the microhardness profile across the joint cross-section into several regions: base material hardness, hardness at the center of the welding interface, hardness in the valley areas, hardness in the peak areas, and hardness in the heat-affected zone. Due to variations in the materials used, the hardness distribution patterns can differ. Typically, for soft metals, the material beneath the valleys of the sonotrode tip exhibits lower hardness compared to that beneath the peaks. However, all these hardness values are higher than those of the original material. This is because plastic deformation at the center of each sonotrode tip peak is more pronounced than beneath the valleys, resulting in significant cold working under each peak. Grain boundaries serve as major barriers to dislocation slip. Finer grains, which form at lower welding energies, provide greater resistance to localized plastic deformation, thus increasing hardness and strength. With increasing welding energy or time, more heat is generated, leading to grain growth and a subsequent reduction in hardness. The observed hardness variation is consistent with the Hall-Petch relationship, as shown in Fig. 19 [67]. Additionally, coarsening and dissolution of strengthening precipitates within the materials can further decrease the hardness at the interface.

Furthermore, Ao et al. [85] investigated the transverse hardness profiles of weld cross-sections subjected to different thermal processing temperatures for 24 hours, as shown in Fig. 20. As the thermal processing temperature increases,

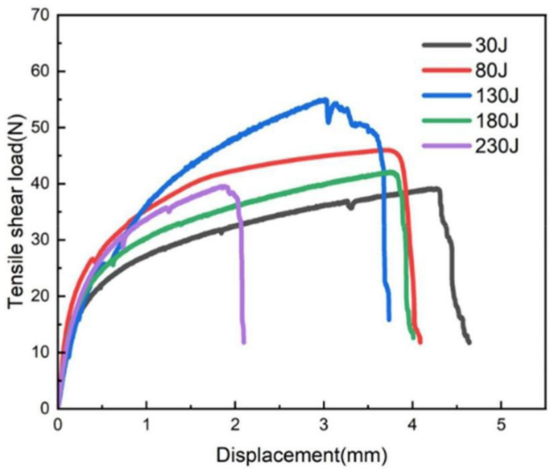

Fig. 18. (Color online) The curves of tensile shear load (N)-displacement (mm) changing with welding energy.

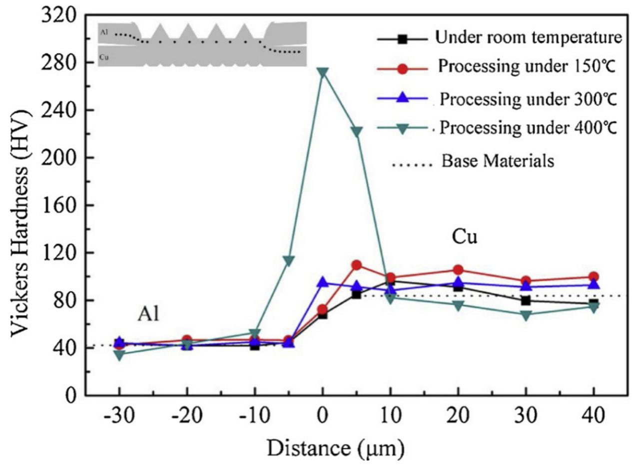

Fig. 20. (Color online) Relationship between the hardness distribution and heating temperatures [85].

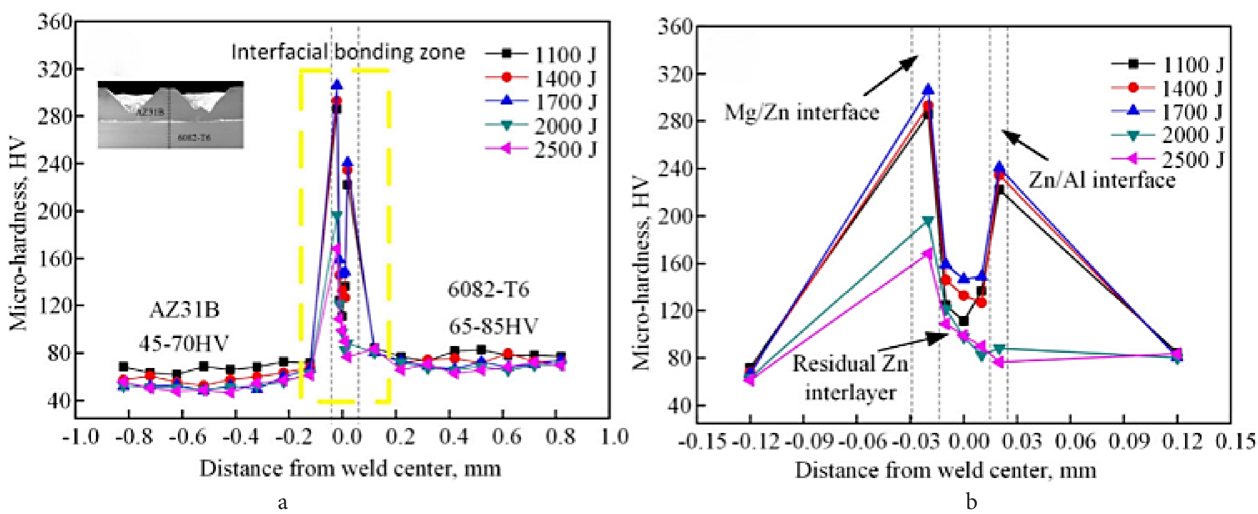

Fig. 19. (Color online) Hardness distributions of the Mg/Al (a) and Mg/Zn/Al (b) joints [67].

the hardness of the Al base metal remains nearly constant, indicating that temperatures below 400°C have no significant effect on its hardness. In contrast, the Cu base metal tends to soften with increasing temperature. Meanwhile, due to the formation of intermetallic compounds, the hardness at the welding interface increases as the heating temperature rises. Under all conditions, the hardness at the joint interface is higher than that of both the Al and Cu base metals, primarily due to the presence of intermetallic compounds.

9. Study of bonding mechanism

Due to the complex thermo-mechanical behavior at the welding interface, the mechanism of USMW for bonding formation remains elusive and lacks a unified conclusion. A large number of researchers have sought to clarify the mechanism of USMW from various perspectives, including the welding process [86–88], grain evolution [87,89], and dislocation slip [90], among others. Bakavos and Prangnell [3], Lee et al. [91] and Zhang et al. [92] investigated USMW of similar metals, and demonstrated that the workpieces were joined by both metallurgical bonding and mechanical interlocking. Zhao et al. [43] observed voids, swirl-like structures, and intermetallic compound layers at the welding interfaces of USMWed Al/Cu joints. They demonstrated that the swirl structures facilitated mechanical interlocking between the materials, thereby enhancing joint strength. Fujii et al. [87] examined the weld formation process in USMWed Cu/Al joints, as shown in Fig. 21. They explained that, at the initial stage of USMW, severe plastic deformation occurs at the welding interface. The oxide layer on the material surfaces is broken down and dispersed into the Al alloy together with some Cu particles. Subsequently, the Al alloy undergoes shear deformation along the direction of ultrasonic vibration. Finally, Cu diffuses into the Al alloy, resulting in metallurgical bonding. The bonding mechanism is analogous to an annealing process following cold work, where instantaneous work hardening and softening occur simultaneously.

Consequently, two major principles of interfacial bonding are recognized during USMW. The first principle posits that high-frequency ultrasonic energy and frictional heat, while insufficient to cause melting, enhance the diffusion rate of molecules or atoms on the outer layers of the welded materials within the welding area, resulting in metallurgical bonding at temperatures below the melting point. The second principle suggests that high-frequency ultrasound, combined with high clamping pressure, induces intense plastic deformation at the contact points within the welding region, generating localized high temperatures that may cause partial melting and ultimately produce a sound joint. Therefore, to better elucidate the mechanisms of interfacial bonding in USMW, more precise temperature measurement devices should be developed. According to Sa et al. [75], plastic deformation is facilitated by the reduction in deformation load and energy requirements due to the acoustic softening effect. As a result, less heat is needed, and the rapid application of ultrasonic energy lowers the static stress of the metals, further promoting the plastic deformation. Watanabe et al. [19] investigated the effect of ultrasonic vibration on the stainless steel joints. Their results demonstrated that ultrasonic vibrations facilitated the formation of equiaxed grains and promoted their accumulation in the center of the weld. The mechanical strength and elongation of the welded section were significantly enhanced with ultrasonic vibration compared to those produced without it. Chen et al. [93] further confirmed that acoustic softening of the material improved plastic deformation, resulting in substantial plastic flow at the welding interface. Consequently, a larger contact surface was formed between the mating sheets, with voids almost entirely eliminated, thereby increasing the mechanical strength.

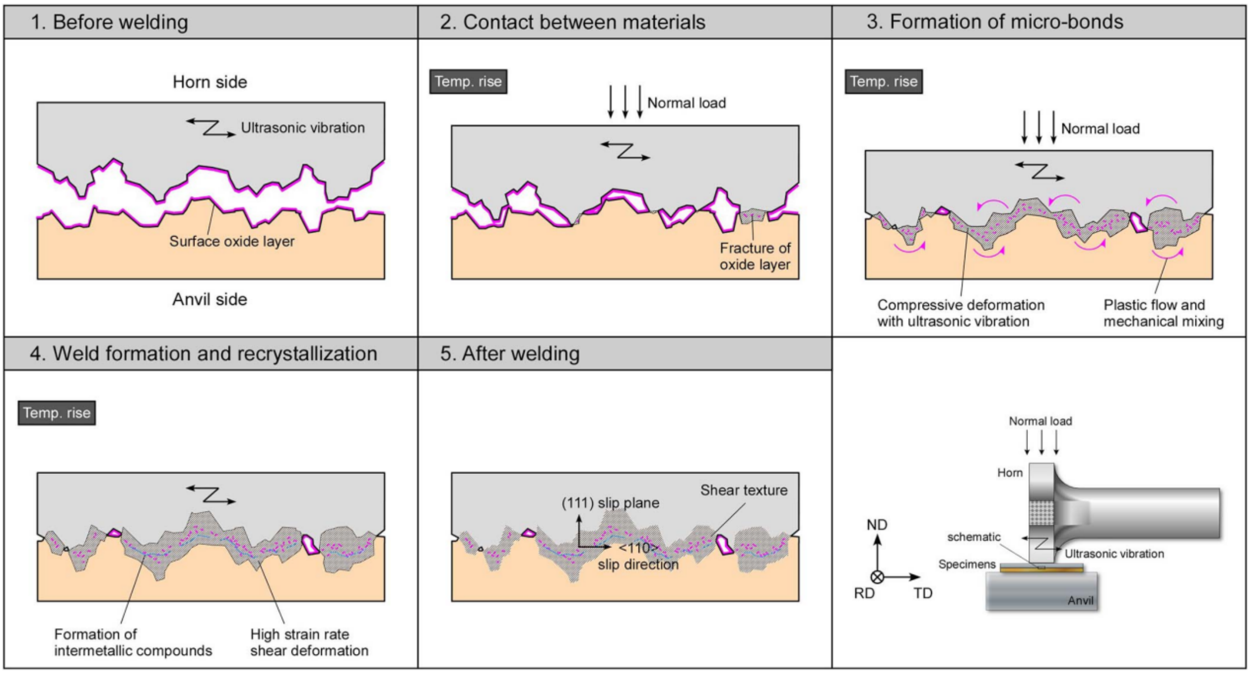

Fig. 21. (Color online) Schematic diagrams of the joint formation process of USMWed Al/Cu joint [87].

The bonding mechanism in USMW consists of several stages. As the vibration continues, interfacial diffusion occurs due to the resulting oscillation, creating a structure that resembles a diffusion weld. A rapid rise in the temperature at the welding interface is followed by plasticization of the metal, completing the welding process without causing melting at the interface. Kelly et al. [94] modeled the acoustic softening effect during ultrasonic consolidation and found that acoustic softening could reduce the yield stress by more than 82%, whereas thermal softening typically reduces yield stress by only about 5%.

10. Conclusions and future trends

This paper reviewed the research status of USMW, including the USMW system and principles, and the enhancement measures for the mechanical performance of USMWed joints, summarized from two aspects: process parameters and material properties. The process parameters include USMW frequency, amplitude, static pressure, welding power, welding energy, welding time, tool design, and welding frequency. The influences of each parameter on the properties of USMWed joints were discussed respectively. In addition, the weldability of materials was evaluated, including hardness, yield strength, thickness, surface roughness, preheating treatment, and other influencing factors. Achieving good bonding requires not only the optimal selection of process parameters, but also improvements in the welding ability of the material during USMW. Furthermore, various viewpoints were considered to account for the bonding mechanism of USMW, with particular attention to the degree of mechanical mixing and material flow, which play important roles in the successful combination of two sheets.

Future research on enhancing joint strength can primarily focus on the following aspects:

1. Study on multi-point welding systems. Currently, most metal ultrasonic spot welding systems are single-point welding systems. In practical production, multiple points often need to be welded on the same workpiece, and the welding sequence will inevitably affect the quality of the joint. Developing a multi-point welding system with coordinated control is of great significance for improving workpiece quality and expanding the application range of welding processes.

2. Establishment of a welding process parameter dataset. There are many factors that influence the strength of ultrasonic welding joints, and the welding parameters vary significantly for different plate thicknesses and materials. The method of determining welding parameters is mostly based on trial and error, which is time-consuming and costly. Establishing a relevant database of welding process parameters is of great guiding significance for reducing production costs and improving production efficiency.

In conclusion, the authors are confident that the rapid advancement of artificial intelligence and machine learning will enable the development of science-based design guidelines for selecting optimal materials and welding process parameters. We anticipate that USMW technology will become increasingly intelligent, with its applications expanding across a broader range of fields.

References

1. Z.L. Ni, J.J. Yang, S. Li, X.X. Wang, F.X. Ye, A review on ultrasonic spot welding of copper alloys, Mater. Sci. Technol. 36 (2020) 264–283.
2. Z.L. Ni, F.X. Ye, Ultrasonic spot welding of aluminum alloys: A review, J. Manuf. Process. 35 (2018) 580–594.
3. D. Bakavos, P.B. Prangnell, Mechanisms of joint and microstructure formation in high power ultrasonic spot welding 6111 aluminium automotive sheet, Mater. Sci. Eng. A 527 (2010) 6320–6334.
4. Z.B. Sun, Z.M. Liang, L.W. Wang, Y. Liu, Y.M. Liang, D.L. Wang, Microstructure and mechanical properties of Al-Zn-Mg-Cu alloy joints welded by ultrasonic spot welding with soft specification, J. Manuf. Process. 116 (2024) 306–314.
5. M.D. Leon, H. Shin, Weldability assessment of Mg alloy (AZ31B) sheets by an ultrasonic spot welding method, J. Mater. Process. Tech. 243 (2017) 1–8.
6. L. Zhou, J. Min, W.X. He, Y.X. Huang, X.G. Song, Effect of welding time on microstructure and mechanical properties of Al-Ti ultrasonic spot welds, J. Manuf. Process. 33 (2018) 64–73.
7. M.P. Satpathy, S.K. Sahoo, Mechanical performance and metallurgical characterization of ultrasonically welded dissimilar joints, J. Manuf. Process. 25 (2017) 443–451.
8. M. Annoni, M. Carboni, Ultrasonic metal welding of AA6022-T4 lap joints: Part I — Technological characterisation and static mechanical behaviour, Sci. Technol. Weld. Joi. 16 (2013) 107–115.
9. K. Nishihara, T. Watanabe, T. Sasaki, Effect of weld tip geometry on ultrasonic welding between steel and aluminum alloy, Adv. Mater. Res. 89–91 (2010) 419–424.
10. D. Lee, W. Cai, The effect of horn knurl geometry on battery tab ultrasonic welding quality: 2D finite element simulations, J. Manuf. Process. 28 (2017) 428–441.
11. S.Q. Xiang, X.F. Zhang, Dislocation structure evolution under electro plastic effect, Mater. Sci. Eng. A 761 (2019) 138026.
12. L.H. Nong, C.H. Shao, T.H. Kim, S.J. Hu, Improving process robustness in ultrasonic metal welding of lithium-ion batteries, J. Manuf. Syst. 48 (2018) 45–54.
13. J.Y. Lin, S. Nambu, K. Pongmorako, T. Koseki, Effect of surface roughness on bonding interface formation of steel and Ni by ultrasonic welding, Sci. Technol. Weld. Join. 25 (2020) 157–163.
14. M.P. Satpathy, S.K. Sahoo, Microstructural and mechanical performance of ultrasonic spot welded Al-Cu joints for various surface conditions, J. Manuf. Process. 22 (2016) 108–114.
15. S. Tokita, C.Y. Liu, Y.S. Sato, Effects of material combination for ultrasonic spot welding on microstructure and strength of Al/Al, Al/Cu, and Al/Ni dissimilar joints, J. Mater. Res. Technol. 26 (2023) 7619–7633.
16. X.M. Cheng, K. Yang, J. Wang, W.T. Xiao, S.S. Huang, Ultrasonic system and ultrasonic metal welding performance: A status review, J. Manuf. Process. 84 (2022) 1196–1216.

17. Q.C. Ma, Y.C. Chao, W.W. Zhang, W.W. Zhao, H.T. Chen, M.Y. Li, Z.M. Liang, Y. Xiao, H.J. Ji, Low energy ultrasonic welding for Cu-Cu joining accelerated via Cu nanoparticles, J. Mater. Process. Tech. 296 (2021) 117210.
18. Z.L. Ni, X.X. Wang, S. Li, F.X. Ye, Mechanical strength enhancement of ultrasonic metal welded Cu/Cu joint by Cu nanoparticles interlayer, J. Manuf. Process. 38 (2019) 88–92.
19. T. Watanabe, S. Yamashita, M. Hiraishi, Effect of surface treatment on the ultrasonic weldability of AZ31B magnesium alloy plate, Keikinzoku 51 (2001) 521–527.
20. D.W. Zhao, D.X. Ren, K.M. Zhao, S. Pan, X.L. Guo, Effect of welding parameters on tensile strength of ultrasonic spot welded joints of aluminum to steel — By experimentation and artificial neural network, J. Manuf. Process. 30 (2017) 63–74.
21. P.G. Mongan, E.P. Hinchy, N.P. O'Dowd, C.T. McCarthy, Optimisation of ultrasonically welded joints through machine learning, Procedia CIRP. 93 (2020) 527–531.
22. Y.Q. Meng, C.H. Shao, Physics-informed ensemble learning for online joint strength prediction in ultrasonic metal welding, Mech. Syst. Signal. Pr. 181 (2022) 109473.
23. J.P. Bergmann, T. Köhler, P. Pöthig, Chapter 7 — Ultrasonic welding, In: Advanced Joining Processes, Elsevier (2021) 239–267.
24. V.K. Patel, S.D. Bhole, D.L. Chen, Influence of ultrasonic spot welding on microstructure in a magnesium alloy, Script. Mater. 65 (2011) 911–914.
25. H.S. Shin, M.D. Leon, Parametric study in similar ultrasonic spot welding of A5052-H32 alloy sheets, J. Mater. Process. Tech. 224 (2015) 222–232.
26. M-N. Feng, Z. Luo, Interface morphology and microstructure of high-power ultrasonic spot welded Mg/Al dissimilar joint, Sci. Technol. Weld. Join. 24 (2019) 63–78.
27. S. Kumar, C.S. Wu, G.K. Padhy, W. Ding, Application of ultrasonic vibrations in welding and metal processing: A status review, J. Manuf. Process. 26 (2017) 295–322.
28. C.Y. Kong, R.C. Soar, P.M. Dickens, Characterisation of aluminium alloy 6061 for the ultrasonic consolidation process, Mater. Sci. Eng. A 363 (2003) 99–106.
29. D.S. Park, H.S. Jang, W.Y. Park, Tensile strength of Cu sheets welded by ultrasonic metal welding, Adv. Mater. Res. 658 (2013) 202–208.
30. J.P. Kumar, Effect of temperature distribution in ultrasonically welded joints of copper wire and sheet used for electrical contacts, Materials 11 (2018) 1010.
31. J.H. Ji, J.Z. Wang, M.Y. Li, Evolution of the bulk microstructure in 1100 aluminum builds fabricated by ultrasonic metal welding, J. Mater. Process. Technol. 214 (2014) 175–182.
32. S. Elangovan, Experimental and theoretical investigations on temperature distribution at the joint interface for copper joints using ultrasonic welding, Manuf. Rev. 1 (2014) 18.
33. M. Baboi, D. Grewell, Evaluation of amplitude stepping in ultrasonic welding. Welding Journal, sponsored by the American welding society and the welding research council, 2010.
34. Z. Al-Sarraf, M. Lucas, A study of weld quality in ultrasonic spot welding of similar and dissimilar metals, J. Phys. 382 (2012) 28–31.
35. Z.q. Zhu, K.Y. Lee, X.L. Wang, Ultrasonic welding of dissimilar metals, AA6061 and Ti6Al4V, Int.J. Adv. Manuf. Technol. 59 (2011) 569–574.
36. M. Shakil, N.H. Tariq, M. Ahmad, M.A. Choudhary, J.I. Akhter, S. S Babu, Effect of ultrasonic welding parameters on microstructure and mechanical properties of dissimilar joints, Mater. Des. 55 (2014) 263–273.
37. H. Li, B. Cao, Effects of welding pressure on high-power ultrasonic spot welding of Cu/Al dissimilar metals, J. Manuf. Process. 46 (2019) 194–203.
38. H. Richter, Investigations into the processes involved when joining together metallic materials by means of ultrasonic welding, Schweiss. Und. Schneid. 22 (1970) 70–3.
39. A. Macwan, A. Kumar, D.L. Chen, Ultrasonic spot welded 6111-T4 aluminum alloy to galvanized high-strength low-alloy steel: Microstructure and mechanical properties, Mater. Des. 113 (2017) 284–296.
40. Y.Y. Zhao, D. Li, Y.S. Zhang, Effect of welding energy on interface zone of Al-Cu ultrasonic welded joint, Sci. Technol. Weld. Join. 18 (2013) 354–360.
41. C. Shao, K.T. Hyung, S.Hu. Jack, J. Jin, A.A. Bell, P.J. Spicer, Tool wear monitoring for ultrasonic metal welding of lithium-ion batteries, J. Manuf. Sci. Eng. 138 (2016) 51005.
42. Y.H. Yang, Y.F. Zhang, Y.D. Cai, Q.Y. Lu, S. Coric, C.H. Shao, Hierarchical measurement strategy for cost-effective interpolation of spatiotemporal data in manufacturing, J. Manuf. Syst. 53 (2019) 159–168.
43. G.P. Liu, X.W. Hu, Y.S. Fu, Y.L. Li, Microstructure and mechanical properties of ultrasonic welded joint of 1060 aluminum alloy and T2 pure copper, Metals 7 (2017) 361.
44. M.A. Murzinova, E.R. Shayakhmetova, A.A. Mukhametgalina, A.A. Sarkeeva, A.A. Nazarov, Local plastic deformation and quality of Cu-Cu joints obtained by ultrasonic welding, Metals 13 (2023) 1661.
45. H. Imai, S.I. Matsuoka, Finding the optimum parameters for ultrasonic welding of aluminum alloys, Jmse.Int. J. 48 (2005) 311–316.
46. H.S. Shin, M.D. Leon, Mechanical performance and electrical resistance of ultrasonic welded multiple Cu-Al layers, J.Mat. Process. Tech. 241 (2017) 141–153.
47. H.S. Shin, M.D. Leon, Analysis of interface solid-state reaction on dissimilar ultrasonic spot welding of Al-Mg alloys, Met. Mater. Int. 23 (2017) 554–561.
48. E.R. Shayakhmetova, M.A. Murzinova, A.A. Nazarov, Ultrasonic welding of nickel with coarse and ultrafine grained structures, Metals 11 (2021) 1800.
49. E.R. Shayakhmetova, M.A. Murzinova, A.A. Mukhametgalina, A.A. Nazarov, Structure evolution in ultrafine-grained nickel induced by ultrasonic welding, Lett. Mater. 14 (2024) 91–96.
50. A.A. Mukhametgalina, Ì.A. Murzinova, A.A. Nazarov, Weld quality and microstructure development in ultrasonically welded titanium joints, Metall. Mater. Trans. A. 53 (2022) 1119–1131.

51. F. W. Müller, A. Schiebahn, U. Reisgen, Quality prediction of disturbed ultrasonic metal welds, J. Adv. Join. Process. 5 (2022) 100086.
52. A. A. Mukhametgalina, E. R. Shayakhmetova, M. A. Murzinova, A. A. Nazarov, A. A. Sarkeeva, Effect of surface state on the quality of copper joints produced by ultrasonic welding, Lett. Mater. 14 (2024) 190–197.
53. K. K. Chen, Y. S. Zhang, Thermal-mechanical analysis of ultrasonic spot welding considering acoustic softening effect, Procedia. Eng. 81 (2014) 2217–2222.
54. H. Huang, J. Chen, J. Cheng, Y. C. Lim, X. H. Hu, Z. L. Feng, X. Sun, Surface engineering to enhance heat generation and joint strength in dissimilar materials AZ31 and DP590 ultrasonic welding, Int. J. Adv. Manuf. Technol. 111 (2020) 3095–3109.
55. Y. Luo, H. Chung, W. Cai, T. Rinker, S. J. Hu, E. Kannatey-Asibu, J. Abell, Joint formation in multilayered ultrasonic welding of Ni-coated Cu and the effect of preheating, J. Manuf. Sci. E-T. Asme 140 (2018) 111003.
56. J. W. Yang, B. Cao, Investigation of resistance heat assisted ultrasonic welding of 6061aluminum alloys to pure copper, Mater. Des 74 (2015) 19–24.
57. S. S. Lee, C. Shao, T. H. Kim, S. J. Hu, E. Kannayey-Asibu, W. Cai, J. P. Spicer, J. A. Abell, Characterization of ultrasonic metal welding by correlating online sensor signals with weld attributes, J. Manuf. Sci. Eng. — T ASME 136 (2014) 051019.
58. Z. L. Ni, F. X. Ye, Dissimilar joining of aluminum to copper using ultrasonic welding, Mater. Manuf. Process. 31 (2016) 2091–2100.
59. H. M. Zhang, Y. J. Chao, Z. Luo, Effect of interlayer on microstructure and mechanical properties of Al-Ti ultrasonic welds, Sci. Technol. Weld. Join. 22 (2017) 79–86.
60. H. Qi, F. X. Ye, H. W. Lu, Visualization of plastic flow in metal ultrasonic welding by adding interlayer, J. Manuf. Process. 83 (2022) 571–575.
61. R. Balasundaram, V. K. Patel, S. D. Bhole, D. L. Chen, Effect of zinc interlayer on ultrasonic spot welded aluminum-to-copper joints, Mater. Sci. Eng. A 607 (2014) 277–286.
62. V. K. Patel, Bhole SD, Chen DL. Microstructure and mechanical properties of dissimilar welded Mg-Al joints by ultrasonic spot welding technique, Sci. Technol. Weld. Join. 17 (2012) 202–206.
63. V. K. Patel, S. D. Bhole, D. L. Chen. Improving weld strength of magnesium to aluminium dissimilar joints via tin interlayer during ultrasonic spot welding, Sci. Technol. Weld. Join. 17 (2012) 342–347.
64. S. S. Ao, M. P. Cheng, W. Zhang, J. P. Oliveira, S. M. Manladan, Z. Zeng, Z. Luo, Microstructure and mechanical properties of dissimilar NiTi and 304 stainless steel joints produced by ultrasonic welding, Ultrasonics 121 (2022) 106684.
65. H. Peng, D. L. Chen, X. F. Bai, X. W. She, D. Y. Li, X. Q. Jiang, Ultrasonic spot welding of magnesium-to-aluminum alloys with a copper interlayer, microstructural evolution and tensile properties, J. Manuf. Process. 37 (2019) 91–100.
66. H. Peng, D. L. Chen, X. F. Bai, P. Q. Wang, D. Y. Li, X. Q. Jiang. Microstructure and mechanical properties of Mg-to-Al dissimilar welded joints with an Ag interlayer using ultrasonic spot welding, J. Magnes. Alloy 8 (2020) 552–563.
67. X. Y. Gu, C. L. Sui, J. Liu, D. L. Li, Z. Y. Meng, K. X. Zhu, Microstructure and mechanical properties of Mg/Al joints welded by ultrasonic spot welding with Zn interlayer, Mater. Des. 181 (2019) 108103.
68. J. Y. Lin, S. Nambu, M. Liu, T. Koseki, Influence of Al and Ni interlayers on interfacial strength evolution during ultrasonic welding of ultra-low-carbon steel and pure Ti, Mater. Sci. Eng. A 798 (2020) 140073.
69. S. S. Dash, S. Biswas, H. Peng, X. Q. Jiang, D. Y. Li, D. L. Chen, Deformation behavior of dissimilar ultrasonic spot-welded joints of a clad 7075 aluminum alloy to galvanized high-strength low-alloy steel, Mater. Sci. Eng. A 894 (2024) 146179.
70. T. Watanabe, H. Itoh, A. Yanagisawa, M. Hiraishi, Ultrasonic welding of heat-treatable aluminium alloy A6061 sheet, Weld. Int. 23 (2009) 633–639.
71. J. J. Yang, Z. L. Ni, A. A. Nazarov, Effect of alcohol on the mechanical and electrical properties of ultrasonic spot welded Cu/Cu joints, Metals 13 (2023) 21.
72. E. Heymann, B. Koehler, Influence of the work piece preparation on ultrasonic Welding, ZIS-Mitteilungen 11 (1969) 180–190.
73. S. Elangovan, S. Semeer, K. Prakasan, Temperature and stress distribution in ultrasonic metal welding — An FEA-based study, J. Mater. Process. Technol. 209 (2009) 1143–1150.
74. H. Li, B. Cao, J. Liu, J. W. Yang, Modeling of high-power ultrasonic welding of Cu/Al joint, Int. J. Adv. Manuf. Technol. 97 (2018) 833–844.
75. A. Siddiq, E. Ghassemieh, Thermomechanical analyses of ultrasonic welding process using thermal and acoustic softening effects, Mech. Mater. 40 (2008) 982–1000.
76. N. G. Shen, A. Samanta, H. T. Ding, W. W. Cai, Simulating microstructure evolution of battery tabs during ultrasonic welding, J. Manuf. Process. 23 (2016) 306–314.
77. J. W. Yang, J. Zhang, J. Qiao, Molecular dynamics simulations of atomic diffusion during the Al-Cu ultrasonic welding process, Materials 12 (2019) 2306.
78. M. Shimaalsadat, B. Franz, M. Bernd, Molecular dynamics simulation of interface atomic diffusion in ultrasonic metal welding, Int. J. Adv. Manuf. Tech. 118 (2021) 2339–2353.
79. A. A. Nazarov, D. V. Bachurin, Z. L. Ni, Atomistic Simulation of Ultrasonic Welding of Copper, Metals 12 (2022) 2033.
80. R. T. Murzaev, M. A. Idrisova, A. A. Nazarov, Simulation of ultrasonic welding of copper: effect of the amplitude of vibrations, Lett. Mater. 14 (2024) 45–50.
81. Y. Q. Meng, M. Rajagopal, G. Kuntumalla, R. Toro, H. Y. Zhao, H. C. Chang, S. Sundar, S. Salapaka, N. Miljkovic, P. Ferreira, S. Sinha, C. H. Shao, Multi-objective optimization of peel and shear strengths in ultrasonic metal welding using machine learning-based response surface methodology, Math. Biosci. Eng. 17 (2020) 7411–7427.
82. P. S. Mantra, B. M. Swayam, K. S. Susanta, Ultrasonic spot welding of aluminum-copper dissimilar metals: a

study on joint strength by experimentation and machine learning techniques, J. Manuf. Process. 33 (2018) 96–110.
83. D. W. Zhao, K. M. Zhao, D. X. Ren, X. L. Guo, Ultrasonic welding of magnesium-titanium dissimilar metals: a study on influences of welding parameters on mechanical property by experimentation and artificial neural network, J. Manuf. Sci. Eng. — T ASME 139 (2017) 031019.
84. Y. H. Yang, C. H. Shao. Hybrid multi-task learning-based response surface modeling in manufacturing, J. Manuf. Syst. 59 (2021) 607–616.
85. S. S. Ao, C. J. Li, W. Zhang, M. P. Wu, Y. Dai, Y. Chen, Z. Luo. Microstructure evolution and mechanical properties of Al/Cu ultrasonic spot welded joints during thermal processing, J. Manuf. Process. 41 (2019) 307–314.
86. X. M. Cheng, K. Yang, S. Z. Liu, S. L. Ji, J. Wang, Effect of ultrasonic welding process parameters on properties of copper conductor joint, Chin. J. Nonferr. Metal. 32 (2022) 3341–3351.
87. H. T. Fujii, H. Endo, Y. S. Sato, H. Kokawa, Interfacial microstructure evolution and weld formation during ultrasonic welding of Al alloy to Cu, Mater. Charact. 139 (2018) 233–240.
88. Y. L. Li, Z. H. Chu, X. W. Li, Y. L. Pan, T. Yamaguchi, W. Q. Wang, Swirl-like Cu-Sn phase formation and the effects on the ultrasonic spot welded joint of Sn-coated Cu plates, J. Mater. Process. Technol. 288 (2021) 116911.
89. J. W. Yang, B. Cao, Q. H. Lu, The effect of welding energy on the microstructural and mechanical properties of ultrasonic-welded copper joints, Materials 10 (2017) 193.
90. Z. J. Zhang, K. F Wang, J. J. Li, Y. Qian, W. Cai, Investigation of interfacial layer for ultrasonic spot welded aluminum to copper joints, Sci. Rep. 7 (2017) 12505.
91. S. S. Lee, T. H. Kim, S. J. Hu, W. W. Cai, J. A. Abell, J. Li, Characterization of joint quality in ultrasonic welding of battery tabs, J. Manuf. Sci. Eng. — T ASME 135 (2013) 021004.
92. C. Q. Zhang, J. D. Robson, P. B. Prangnell, Dissimilar ultrasonic spot welding of aerospace aluminum alloy AA2139 to titanium alloy TiAl6V4, J. Mater. Process. Tech. 231 (2016) 382–388.
93. K. K. Chen, Y. S Zhang, H. Z. Wang, Effect of acoustic softening on the thermal-mechanical process of ultrasonic welding, Ultrasonics 75 (2017) 9–21.
94. G. S. Kelly, S. G. Advani, J. W. Gillespie, T. A. Bogetti, A model to characterize acoustic softening during ultrasonic consolidation, J. Mater. Process. Tech. 213 (2013) 1835–1845.